



Timing and magnitude of future annual runoff extremes in contrasting Alpine catchments in Austria

Sarah Hanus^{1,2}, Markus Hrachowitz¹, Harry Zekollari^{1,3}, Gerrit Schoups¹, Miren Vizcaino¹, and Roland Kaitna⁴

¹Faculty of Civil Engineering and Geosciences, Delft University of Technology, Stevinweg 1, 2628 CN Delft, the Netherlands

²Department of Geography, University of Zurich, Zurich, CH-8006, Switzerland

³Laboratoire de Glaciologie, Université libre de Bruxelles, Brussels, Belgium

⁴Institute of Mountain Risk Engineering, University of Natural Resources and Life Sciences, Vienna, Austria

Correspondence: Sarah Hanus (sarah.hanus@geo.uzh.ch)

Abstract. Hydrological regimes of alpine catchments are expected to be strongly affected by climate change mostly due to their dependence on snow and ice dynamics. While seasonal changes have been studied extensively, studies on changes in the timing and magnitude of annual extremes remain rare. This study investigates the effects of climate change on runoff patterns in six contrasting alpine catchments in Austria using a process-based semi-distributed hydrological model and projections from 14 regional climate and global climate model combinations for RCP 4.5 and RCP 8.5. The study catchments represent a spectrum of different hydrological regimes, from pluvial-nival to nivo-glacial, as well as distinct topographies and land forms, characterizing different elevation zones across the Eastern Alps to provide a comprehensive picture of future runoff changes. The climate projections are used to model river runoff in 2071–2100, which are then compared to the 1981–2010 reference period for all study catchments. Changes in timing and magnitude of annual maximum and minimum flows as well as in monthly runoff and snow melt are quantified and analyzed. Our results indicate a substantial shift to earlier occurrences in annual maximum flows by 9 to 31 days and an extension of the potential flood season by one to three months for high-elevation catchments. For low-elevation catchments, changes in timing of annual maximum flows are less pronounced. Magnitudes of annual maximum flows are likely to increase by 2–18% under RCP 4.5, while no clear changes are projected for four catchments under RCP 8.5. The latter is caused by a pronounced increase in evaporation and decrease in snow melt contributions which offset increases in precipitation. Minimum annual runoff occur 13–31 days earlier in the winter months for high-elevation catchments, whereas for low-elevation catchments a shift from winter to autumn by about 15–100 days is projected. While all catchments show an increase in mean magnitude of minimum flows by 7–30% under RCP 4.5, this is only the case for four catchments under RCP 8.5. Our results suggest a relationship between the elevation of catchments and changes in timing of annual maximum and minimum flows. For the magnitude of the extreme flows, a relationship is found between catchment elevation and annual minimum flows, whereas this relationship is lacking between elevation and annual maximum flow.



1 Introduction

The hydrological cycle is impacted by climate change due to rising temperatures and changing precipitation patterns (Cramer et al., 2014; IPCC, 2019). Higher temperatures lead to rising atmospheric water demand and changes in snow and ice dynamics which both affect runoff processes. Changes in runoff patterns can be observed for the past, e.g. trends in timing and magnitude of floods (Blöschl et al., 2017, 2019) and subseasonal trends in runoff (Kormann et al., 2015). As reiterated by the latest IPCC report (IPCC, 2019), special attention needs to be given to high-elevation areas as their hydrological regimes are strongly influenced by snow dynamics and changes in glaciated areas. Furthermore, the average temperature increase in the Alps over the last century was by a factor 1.6 higher than the average worldwide temperature increase over land (IPCC, 2007; Brunetti et al., 2009). In alpine regions, monthly runoff and the associated occurrence of flow extremes are characterized by a strong seasonality with maximum runoff typically occurring in spring and summer during the snow melt season and minimum runoff in winter. Changes in flow magnitudes and seasonality in alpine environments can have wide-reaching socio-economic and ecological implications, ranging from hydro-power production (e.g., Schaeffli et al., 2019; Hakala et al., 2020) over water availability (Barnett et al., 2005; Brunner et al., 2019b) to flood risk and ecosystem functioning (Cauvy-Fraunié and Dangles, 2019). Hence, it is important to assess future changes in seasonal runoff patterns. Over the past decades observations provided evidence of positive trends in spring runoff magnitudes and negative trends in summer runoff in the Alpine region, with timing of trends largely depending on elevation (Kormann et al., 2015). Similarly, Laaha et al. (2016) report positive trends in high-alpine low flows over the past.

To investigate potential impacts of future climate change on hydrology, hydrological models can be run with projected forcing data generated by regional climate models (RCMs) for different emission scenarios. This approach has previously been widely used, also in the Alpine region. Snow mass and snow cover duration are expected to decline in the Alps in future (Laghari et al., 2012; Bavay et al., 2013; Marty et al., 2017), and so are its glaciers, which are projected to largely disappear during the 21st century (Zekollari et al., 2019). As a result, summer low flows are expected to decrease in catchments in Switzerland (Jenicek et al., 2018; Muelchi et al., 2021). However, annual low flows are projected to increase in the Alps as winter low flows increase due to changes in snow dynamics related to increased temperatures (Laaha et al., 2016; Parajka et al., 2016; Marx et al., 2018; Laurent et al., 2020; Muelchi et al., 2021). With respect to annual floods in high alpine catchments, studies disagree on the sign of change, suggesting future increases (Köplin et al., 2014) or decreases (Muelchi et al., 2021) in magnitude.

In Austria, studies project an increase in winter flows and a decrease in summer flows in the 21st century (Laghari et al., 2012; Tecklenburg et al., 2012; Goler et al., 2016; Hanzer et al., 2018; Holzmann et al., 2010) with the largest increases in winter flows found in high-elevation areas (Stanzel and Nachtnebel, 2010). For the spring runoff, an inconsistent future trend over Austria is projected, with increases in high alpine areas in Western Austria (Stanzel and Nachtnebel, 2010; Tecklenburg et al., 2012) and decreases elsewhere (Laghari et al., 2012). Holzmann et al. (2010) assessed changes in future high flows, showing a decrease in high flows in Western Austria and an increase in Eastern Austria. Goler et al. (2016) determined a decrease of the number of days of low runoff in winter and an increase in summer in Austria.



55 So far, climate change impact studies on hydrology using an ensemble of climate simulations are limited in the Austrian Alps.
However, using simulations of different general circulation models (GCMs) and RCMs is essential to quantify the uncertainty
introduced by climate change simulations and to limit the potential for misinterpretations (Addor et al., 2014; Her et al.,
2019). To our knowledge, the study by Laghari et al. (2012) implements the largest number of climate models (13), but only
investigates impacts on a single catchment in Austria. Furthermore, previous studies mostly analyzed one single aspect of
60 runoff (monthly, low or high flows) or one signal (magnitude or timing), but lack an extensive overview of future changes in a
range of mountainous catchments. An exception is a recent study in the Swiss Alps by Muelchi et al. (2021) and the study by
Blöschl et al. (2011) in the Austrian Alps, but the latter analysis is based on modifying future hydrological mechanisms, rather
than using GCMs and representative concentration pathways (RCPs) for representing future climate.

To cover this gap, in this study, past (1981–2010) and future (2071–2100) flow magnitudes and timing are quantified by
65 running a process-based hydrological model in six meso-scale alpine catchments with contrasting hydro-climatic regimes and
topography. The future climate is derived from an ensemble of 14 climate simulations for RCP 4.5 and RCP 8.5. The overall
objective of this study is to provide a comprehensive overview of potential future changes in runoff dynamics across the Eastern
Alps. More specifically, we are testing the hypothesis that future changes in magnitude and timing of annual runoff extremes
differ between high- and low-elevation catchments and place these observations in a general context by directly comparing
70 them to other simulated future runoff changes from neighboring countries.

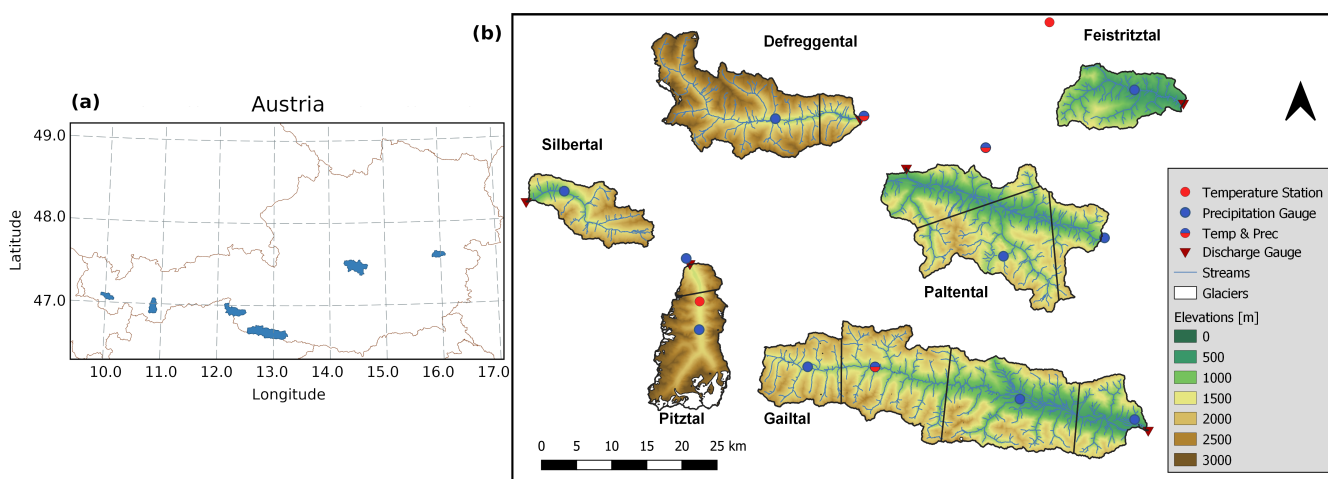


Figure 1. (a) Location of the six study catchments in Austria (shaded blue area), (b) elevation maps of the study catchments including the location of precipitation and temperature observation stations, as well as the division into precipitation zones (black lines).



Table 1. Catchment characteristics. Precipitation and temperature are based on data from 1986-2010 used in this study. Runoff coefficients are based on simulations of this study. The runoff regimes are based on Mader et al. (1996).

	Silbertal	Pitztal	Defreggental	Gailtal	Paltental	Feistritzal
Area [km ²]	100	166	267	587	370	116
Elevation [m]	671-2764	1339-3763	1096-3485	596-2778	633-2447	449-1595
Mean Altitude[m]	1776	2558	2233	1476	1315	917
Yearly mean precipitation[mm year ⁻¹]	1423	915	926	1313	1213	875
Yearly mean runoff coefficient [-]	0.68	0.58	0.60	0.66	0.57	0.36
Yearly mean temperature [°C]	2.8	-1.2	-1.3	3.3	4	6.9
Runoff Regime	nival	nivo-glacial	nival	autumn nival	moderate nival	nivo-pluvial
Bare (Glacier) [%]	20 (0)	70 (18)	43 (1.5)	8 (0)	4 (0)	0 (0)
Grass [%]	46	23	32	33.5	32	25
Forest [%]	32	6	23	56.5	61	72
Riparian [%]	2	1	2	2	3	3
No. Prec. Gauges	1	2	2	4	3	1

Table 2. EURO-CORDEX models used for this study (Jacob et al., 2014), model resolution 12.5x12.5 km, rip index refers to realization, initialization method and physics version used for GCM.

ID	GCM	RCM
1	CNRM-CM5 rli1p1	CCLM4-8-17
2	CNRM-CM5 rli1p1	ALADIN53
3	CNRM-CM5 rli1p1	RCA4
4	EC-EARTH rli1p1	RACMO22E
5	EC-EARTH r3i1p1	HIRHAM5
6	EC-EARTH r12i1p1	CCLM4-8-17
7	EC-EARTH r12i1p1	RCA4
8	CM5A-MR rli1p1	WRF361H
9	CM5A-MR rli1p1	RCA4
10	HadGEM2-ES rli1p1	CCLM4-8-17
11	HadGEM2-ES rli1p1	RCA4
12	HadGEM2-ES rli1p1	RACMO22E
13	MPI-ESM-LR rli1p1	CCLM4-8-17
14	MPI-ESM-LR rli1p1	RCA4



2 Methodology

2.1 Study site and data

For this study, six meso-scale catchments with different elevation ranges and hydrological regimes in the Austrian Alps are chosen (Fig. 1; Table 1). The Pitztal is the highest catchment with a mean elevation of 2558 m and a nivo-glacial regime with 18 % glacial coverage. In contrast, the lowest catchment, Feistritzal (917 m) in the Pre-Alps, has a nivo-pluvial hydrological regime. The other catchments have a nival regime and range in mean elevation from 1315 m (Paltental) to 2233 m (Defreggental), with limited glacial coverage. High-elevation catchments (Silbertal, Defreggental, Pitztal) consist mainly of bare rock and grassland, whereas more than half of the low-elevation catchments (Feistritzal, Paltental, Gailtal) is covered by forests (Table 1).

Daily runoff sums are taken from the Hydrographic Service Austria (<https://ehyd.gv.at/>) (1985–2015). Temperature and precipitation data are made available from Austrian Central Institute for Meteorology and Geodynamics (ZAMG) and the Hydrographic Service Austria (1980–2015) (Fig. 1). Precipitation data is aggregated and temperature data averaged to a daily resolution. The long-term water balance of each catchment is computed to check the plausibility of the data. Since the long-term precipitation for the Defreggental and Silbertal is lower than long-term runoff, the measured runoff is scaled such that the long-term water balance matches the Budyko framework. Hereby, we decided to scale the runoff data rather than the precipitation data, because precipitation of climate simulations match historical precipitation observations and this study focuses on changes in runoff rather than absolute values. Using this approach, climate simulations can be left unchanged. Daily potential evaporation is estimated based on daily temperature and potential sunshine hours using the Thornthwaite method (Thornthwaite, 1948; Oudin et al., 2005)

Land use types of the catchments are determined using the CORINE Land Cover data set from 2018 (<https://land.copernicus.eu/pan-european/corine-land-cover>) and the riparian zone is determined based on a 10 × 10m height-above-nearest drainage map (HAND) (Gharari et al., 2011). Glacier outlines of the past are taken from the Austrian Glacier Inventory (Lambrecht and Kuhn, 2007; Abermann et al., 2010). A linear interpolation between the observation years is applied and the change in glacial area between 1997 and 2006 is extrapolated to 2015. Zekollari et al. (2019) simulate the future evolution of glaciers in Europe with GloGEMflow, a recent extension of the Global Glacier Evolution Model (Huss and Hock, 2015) that considers ice flow explicitly. Future simulated glacier extents in the Pitztal under different emission scenarios are used in this study. These are scaled to match the extrapolated glacier areas in 2015.

Daily gridded snow cover data for the 2000–2015 period from the MODIS satellite product MOD10A1 (Hall and Riggs, 2016) is used, in addition to the daily runoff data for the calibration of the hydrological model. Moreover, a 10x10 m digital elevation model of Austria (<https://www.data.gv.at/katalog/dataset/dgm>) is used to derive topographic information.

In addition, past and future temperature and precipitation estimates at the station scale are obtained for the 1981–2010 and 2071–2100 periods from 14 high-resolution climate simulations generated based on the EURO-CORDEX data set (Jacob et al., 2014) (Table 2) and bias-corrected using scaled distribution mapping to remove systematic model errors, for the two emission



scenarios RCP4.5 and RCP8.5 (Switanek et al., 2017). The simulations provide temperature and precipitation data on a daily
 105 basis at the station scale corresponding to the location of precipitation and temperature stations (Fig.1) (Switanek et al., 2021).

Table 3. Relevant water balance and constitutive equations of the hydrological model, **Reservoirs/States [mm]**: S_{fast} : fast responding reservoir, $S_{glacier}$: glacier reservoir, S_{int} : interception reservoir, S_{slow} : slow responding reservoir, S_{snow} : snow reservoir, S_u : soil reservoir. **Fluxes [mm day⁻¹]**: E_{int} : interception evaporation, E_u : evapotranspiration, M_{tot} : melt, P : precipitation, P_{snow} : precipitation as snow, $P_{eff,(tot)}$: (total) effective precipitation, q_{base} : base flow, q_{fast} : fast runoff, q_{over} : overland flow, q_{pref} : preferential flow, q_{rip} : capillary rise riparian zone. **Parameters**: β [-]: factor accounting for nonlinearity, F_{evap} [-]: evapotranspiration control factor, F_{melt} [mm °C⁻¹]: melt factor, I_{max} [mm]: max. interception capacity, k_{fast} [day⁻¹]: fast hillslope constant, $k_{fast,rip}$ [day⁻¹]: fast riparian constant, k_{slow} [day⁻¹]: slow constant, M_M [°C]: smoothness parameter for melt, ρ_p [-]: share preferential flow, ρ_{rip} [-]: share riparian flow, $S_{u,max}$ [mm]: max. soil storage capacity, T_{thresh} [°C]: threshold temperature for precipitation partitioning and melt. $area_{gl}$: glaciated area. A detailed model description can be found in Supplementary Material S1.

Reservoir	Water balance equation	Constitutive functions
Interception	$\frac{dS_{int}}{dt} = P_{rain} - E_{int} - P_{eff}$	1) $P_{eff} = \max(S_{int} - I_{max}, 0) \cdot dt^{-1}$ 2) $E_{int} = \min(0.5 \cdot E_{pot}, S_{int} \cdot dt^{-1})$
Snow	$\frac{dS_{snow}}{dt} = P_{snow} - M_{snow}$	3) $M = F_{melt} \cdot M_M \left(\frac{T - T_{thresh}}{M_M} + \ln(1 + \exp(-\frac{T - T_{thresh}}{M_M})) \right)$ 4) $M_{snow} = \min(M, S_{snow} \cdot dt^{-1})$ 5) $M_{glacier} = M$ 6) $M_{tot} = M_{snow} \cdot (1 - area_{gl}) + M_{glacier} \cdot area_{gl}$
Unsaturated Zone	$\frac{dS_u}{dt} = q_u - E_u$	7) $P_{eff,tot} = \sum_{i=1}^{Elevations} P_{eff} + \sum_{i=1}^{Elevations} M_{tot}$ 8) $C_r = 1 - (1 - \frac{S_u}{S_{u,max}})^\beta$ 9) $q_u = \min((1 - C_r) \cdot P_{eff,tot}, (S_{u,max} - S_u) \cdot dt^{-1})$ 10) $q_{u,rip} = \min((1 - C_r) \cdot (P_{eff,tot} + q_{rip}), (S_{u,max} - S_u)) \cdot dt^{-1}$ 11) $E_u = (E_{pot} - E_{int}) \cdot \min(\frac{S_u}{S_{u,max} \cdot F_{evap}}, 1)$
Fast Reservoir	$\frac{dS_{fast}}{dt} = q_{overland} - q_{fast}$	12) $q_{overland} = (P_{eff,tot} - q_u) \cdot \rho_p$ 13) $q_{overland,rip} = P_{eff,tot} + q_{rip} - q_{u,rip}$ 14) $q_{fast} = k_{fast} \cdot S_{fast}$
Slow Reservoir	$\frac{dS_{slow}}{dt} = \sum_{i=1}^{HRU} q_{pref} - q_{slow}$	15) $q_{pref} = (P_{eff,tot} - q_u) \cdot (1 - \rho_p)$ 16) $q_{slow} = k_{slow} \cdot S_{slow}$

2.2 Hydrological model

2.2.1 Model structure

A semi-distributed process-based hydrological model is used to model the runoff behaviour of the catchments. The model is based on hydrological response units (HRUs) as utilized and described for example by Gao et al. (2014) and Prenner et al.

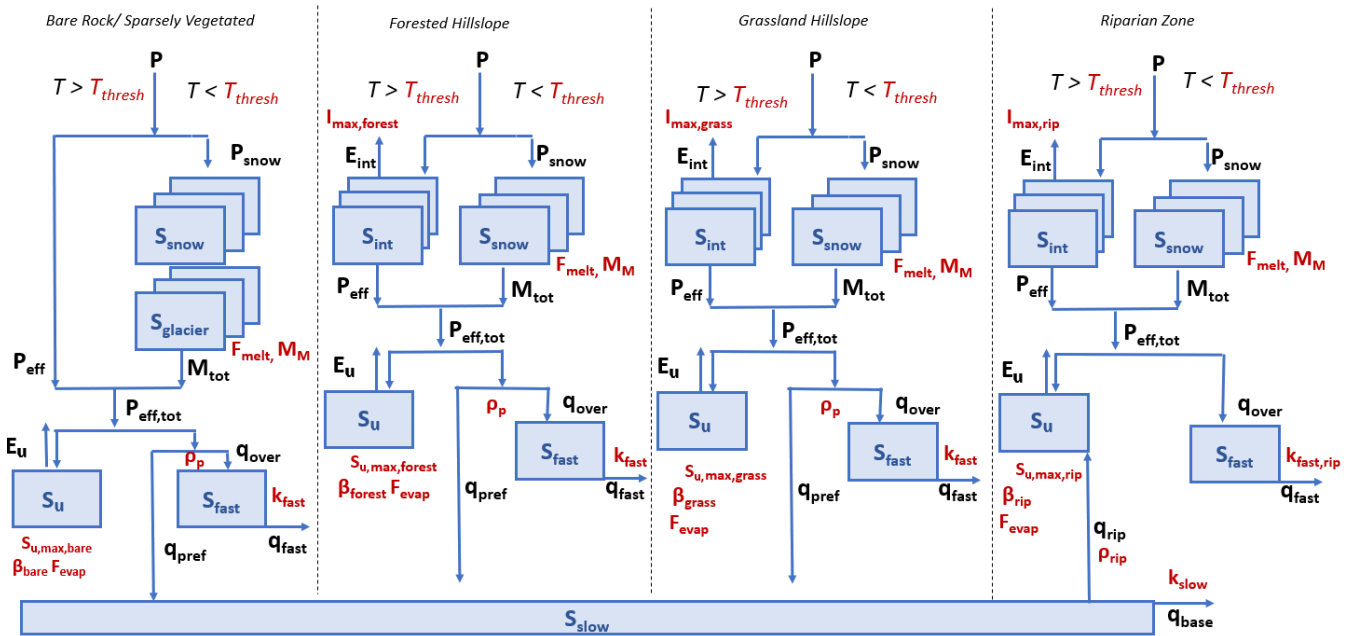


Figure 2. Schematic representation of model structure per precipitation zone, showing model states (blue), fluxes (black) and parameters (red).

110 (2018). The aim is to represent dominant physical processes in the catchment based on topography and land cover classes while limiting model complexity (Savenije, 2010). A detailed model description is given in the Supplementary Material S1. Briefly, the following storage reservoirs are included in the model and represented by the water balance equations (Table 3): snow, interception, unsaturated root zone as well as a fast and a slow responding groundwater component. In total, the model is implemented with a hierarchy of three levels of spatial resolution which are, in ascending resolution, (i) one to four precipitation
 115 zones per catchment (Fig. 1), (ii) the four HRUs per precipitation zone (cf. Table 1) and (iii) individual 200 m elevation zones per HRU (e.g., Roodari et al., 2020).

More specifically, the division of catchments into precipitation zones is based on available precipitation gauges using Thiessen polygons (Fig. 1). The model is run separately for each precipitation zone with different precipitation input. Catchment-scale model outputs are then obtained for each time step as the area-weighted aggregated outputs of the individual precipitation
 120 zones. In each precipitation zone the model is further discretized into four HRUs (Fig. 2): bare rock, forest, grassland and riparian zone. To account for differences in vegetation cover in the individual HRUs, the vegetation dependent model parameters I_{max} and $S_{u,max}$, representing the water storage capacities in interception and root zone storage reservoirs, were allowed to vary between HRUs. All other parameters are kept constant across HRUs to minimize the number of calibration parameters. Note that interception storage is considered to be negligible in the bare rock HRU. Therefore I_{max} is set to 0, which removes
 125 that storage from the bare rock HRU (Fig. 2). In contrast to the other HRUs, the riparian zone includes the process of upwelling groundwater (q_{rip}) to sustain soil moisture throughout dry seasons (Prenner et al., 2018; Hulsman et al., 2020). Glaciers are



130 incorporated in the model as an unlimited snow reservoir in the bare rock unit according to their areal extent (Seibert and
 Vis, 2012; Mostbauer et al., 2018). To allow for elevation-dependent snow dynamics the HRUs are further stratified into 200
 m elevation zones. Snow accumulation and melt in the individual elevation zone is estimated with an improved degree-day
 method as suggested by Girons Lopez et al. (2020).

2.2.2 Calibration & evaluation

In total, 20 parameters must be calibrated for each catchment, except for the Pitztal, where an additional loss term is imple-
 mented to account for artificial diversion of water through a pipe-system from the catchment for hydropower generation. All
 model parameters, including their uniform prior distributions and the ranges of the parameter sets retained as feasible after
 135 calibration, are given in Supplementary Material Table S1. The parameter combinations of the individual HRUs are a priori
 constrained based on relational process-constraints as suggested by Gharari et al. (2014) and similarly implemented for the
 study catchments by Prenner et al. (2019) (Supplementary Material S2) to ensure process consistency and to limit the ef-
 fects of equifinality. For a robust representation of model-internal dynamics, we further adopt an extended multi-objective and
 multi-variable calibration strategy. (e.g., Efstratiadis and Koutsoyiannis, 2010). To do so we train the model to simultaneously
 140 optimize eight objective functions, describing different signatures of flow, as well as the presence of snow cover (Table 4).
 Detailed descriptions of the signatures and objective functions are provided in Supplementary Material S3. The overall model
 performance is assessed by an objective function based on the mean Euclidean distance from the theoretical “perfect model”

(e.g., Hrachowitz et al., 2014; Hulsman et al., 2020): $Obj_{tot} = 1 - \sqrt{\frac{\sum_{n=1}^N (1 - Obj_n)^2}{N}}$ where 1 indicates a perfect model. To ensure
 145 balanced solutions and in the absence of more detailed information, the individual objective functions were equally weighted
 to compute Obj_{tot} .

Table 4. Signatures & the associated objective functions (Obj_n) used for model calibration and post-calibration model evaluation, including
 the Nash Sutcliffe Efficiency (E_{NSE}), the volumetric error (E_{VE}) and the relative and absolute error (E_{RE} , E_{AE}).

Signature	Abbreviation	Objective Function	Reference
Timeseries of Flow	Q	$E_{NSE,Q}$	(Nash and Sutcliffe, 1970)
		$\bar{E}_{NSE,\log(Q)}$	(Nash and Sutcliffe, 1970)
		$E_{VE,Q}$	(Criss and Winston, 2008)
Flow Duration Curve	FDC	$E_{NSE,FDC}$	(Euser et al., 2013)
Autocorrelation	AC1	$E_{RE,AC1}$	(Euser et al., 2013)
	AC90	$E_{NSE,AC90}$	(Hrachowitz et al., 2014)
Monthly Runoff Coefficient	RC	$E_{NSE,RC}$	(Hrachowitz et al., 2014)
Snow Cover	SC	$E_{AE,SC}$	(Finger et al., 2015)



The models are calibrated using in situ observations of precipitation, temperature and runoff with a Monte Carlo sampling scheme based on three million realizations for each catchment. Calibration is run for a period of 20 years (Oct. 1985–Oct. 2005) with a prior warm-up period of three years.

150 After calibration, the models are evaluated using the available flow data after the calibration period (November 2005–2013/
2015, depending on the catchment). For the post-calibration model evaluation, the same objective functions as for calibration
were used. To partially capture model uncertainty but limit the amount of data for further analysis, the best 0.01% of the
calibrated parameter sets (300 sets) based on Obj_{tot} during calibration were used for further analysis with an additional
constraint of $Obj_{tot} > 0.8$ during calibration. This decision allows an ensemble analysis of plausible solutions, based on
the concept of equifinality, suggesting that observed hydrological response dynamics can be reproduced by many different
155 parameter sets (Beven and Binley, 1992).

2.3 Climate simulations as model input

To analyze the effect of a changing climate on the hydrological response, the model was run using climate simulations for a 30-
year period in the past (1981–2010) and a period at the end of the 21st century (2071–2100). The modelled flow characteristics,
i.e. the model output, for the two individual 30-year periods were then quantitatively compared. While the climate simulations
160 for the calibration period match the statistical distribution of the hydro-climatic drivers, they do not match their timing. In other
words, the simulations of past precipitation and temperature are not concomitant with the in situ observations of flow at the
daily time scale of the model application. Therefore, the model had to be calibrated using in situ observations (Section 2.2). To
use the calibrated model parameters in a meaningful way in combination with the simulations of the past and future, we first
test whether the long-term distributions of the in situ data and the modelled climate for the 1981–2010 period are equivalent to
165 avoid misinterpretation of the model results. In addition, we also compare the long-term distributions of modelled flow using
both in situ and simulated hydro-meteorological input for the 1981–2010 period to assess presence of potential systematic
errors. After these tests of data equivalence, we generate 300 model simulations using the parameter sets retained as “best”
(Section 2.2) for each of the 14 individual climate simulations (Table 2) for each of the two emission scenarios (RCP4.5 and
RCP8.5; Section 2.1) for both the 1981–2010 and the 2071–2100 periods. In total this results in a total of 100.000 individual
170 30-year daily model realizations. While the glacier extent in the Pitztal catchment is adapted over time as described in Section
2.1 and the glacier extent in the Defreggental catchment is assumed to be negligible for the future period, the other HRUs are
kept constant over time.

2.4 Analysis of change

Simulations of past and future runoff are compared for the same climate simulation and parameter set, using averages over the
175 30-year time period. The methods to analyze changes in extreme flows are briefly described in the following sections (refer to
the Supplementary Material S4 for equations).



2.4.1 High flows

For investigating the changes in high flows, an approach similar to Blöschl et al. (2017, 2019) is taken. We generate time series comprising the highest modeled peak flow for each calendar year, i.e. the annual maximum flow (AMF). For analyzing the change in magnitudes of high flows, the relative and absolute changes in the mean AMF between the past and the future are quantified for each simulation. In addition, the magnitudes of each year are ranked and the exceedance probability is calculated. The absolute changes in magnitude for a certain return period, related to an exceedance probability, are calculated per simulation. For computing the mean timing of high flows over the two individual 30-year periods, the method of circular statistics is used (e.g., Young et al., 2000; Blöschl et al., 2017). This method computes time differences between events correctly despite turns of the year. Nevertheless, a bimodal flood season would be hidden by this approach, as the average date of occurrence would be located between the two seasons. Therefore, additionally the distribution of timing in the two 30-year periods is analyzed by computing the relative frequencies of AMF occurring within individual 15-day periods. A 15-day period is chosen to allow observations of relatively small change over time while being long enough for multiple events to co-occur in the same period.

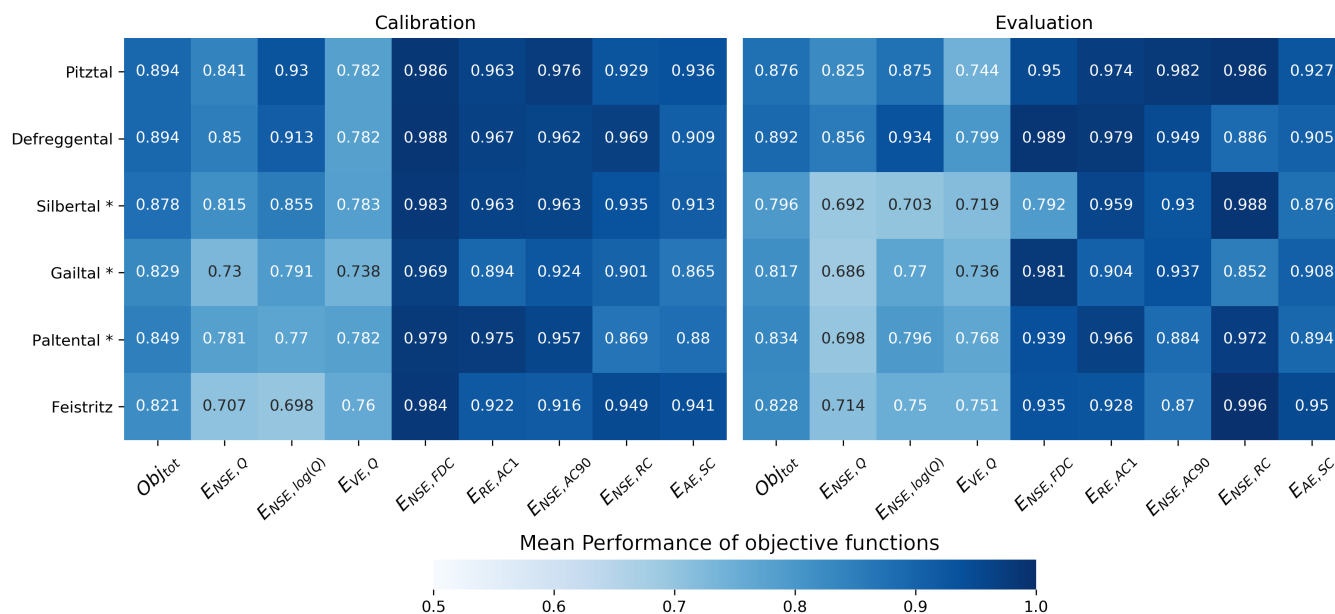


Figure 3. Mean model performance of the best 300 parameter sets for the calibration and evaluation periods. Obj_{tot} shows the overall model fit, * indicates the catchments that use eight years of evaluation instead of ten.

2.4.2 Low flows

Changes in low flows are analyzed using the annual minimum average runoff of seven consecutive days. This minimum average runoff is computed using a moving average from June to May to avoid complications with turns of the year as low



flows are expected mainly in winter (Vormoor et al., 2017; Jenicek et al., 2018). The mean timing over the two individual
30-year periods and the distribution of timing in these periods are computed with the same approach as for high flows, i.e.
195 using circular statistics.

3 Results

3.1 Hydrological model calibration and evaluation

Overall, the models reproduce the main features of the observed hydrological response for both the calibration and the evalu-
ation periods in all study catchments with $Obj_{tot} = 0.82$ – 0.89 and 0.80 – 0.89 , respectively (Fig. 3). The model performance
200 with respect to the individual objective functions remains relatively stable between the calibration and evaluation periods with,
for example, $E_{NSE,Q} = 0.71$ – 0.85 only experiencing very minor reductions to 0.69 – 0.86 (3). Closer inspection of the
modelled hydrographs indicates that the short-term flow dynamics are generally adequately captured (Fig. 4; Fig. S1-S12).
However, in some cases, peak flows that are in most cases likely to be associated with very localized, high-intensity convective
rainfall events, remain underestimated due to uncertainties in precipitation observations (Hrachowitz and Weiler, 2011). In
205 contrast, the modelled mean regime curves of flow over the combined calibration and evaluation periods match the observa-
tions rather well (Fig. 5), indicating that the models adequately capture the general magnitudes and seasonal pattern in all study
catchments.

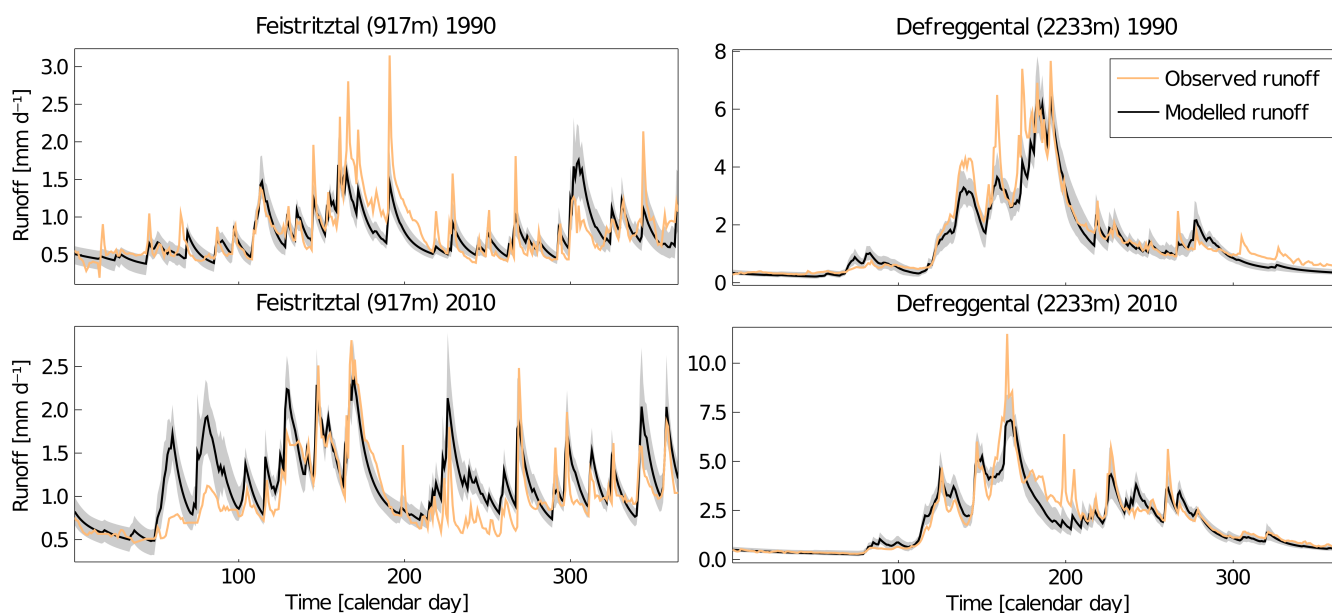


Figure 4. Comparison of measured and modelled runoff for a year during calibration period (1990) and year during the evaluation period (2010). The black line indicates mean modelled runoff using best parameter sets, the shaded area corresponds to the range of best parameter sets.

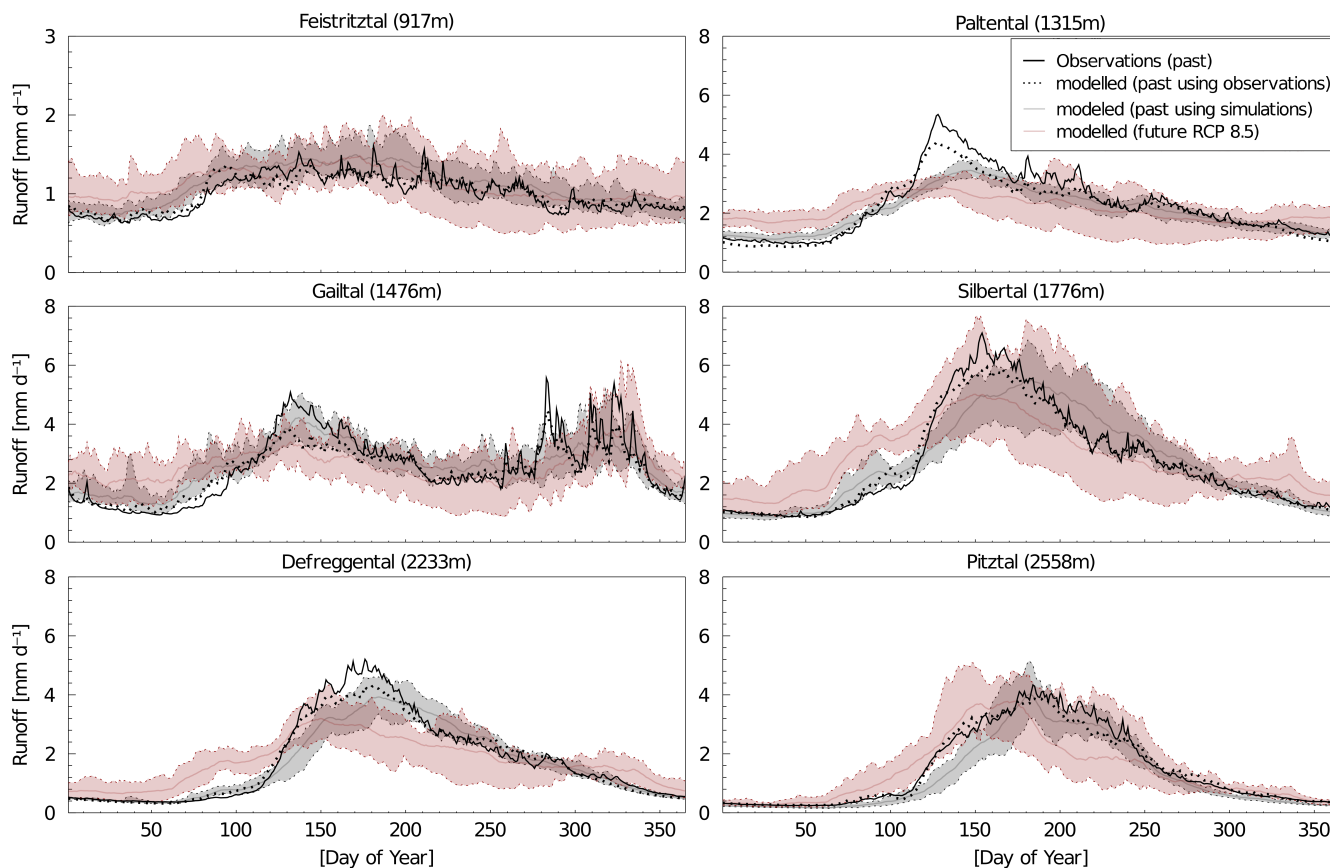


Figure 5. Comparison of observed (black line) and modelled runoff regime in past (1985–2013) using meteorological observations (dotted line) as well as runoff regimes modelled by climate simulations in past (1981–2010) and future (2071–2100) for RCP 8.5 (line represents the mean flow regime within the range of 14 climate models (shaded area). Note that the extent of the y-axis differs for the Feistriztal.

3.2 Simulation of historical climate and hydrology

The seasonality of precipitation and temperature of climate simulations in the period 1981–2010 closely matches the seasonality of the measured station data. For the high-elevation catchments (Silbortal, Defreggental, Pitztal), the climate models slightly underestimate the monthly temperatures, mostly in the summer months (e.g. Silbortal catchment in Fig. 6 and other catchments in Fig. S13-17). The seasonality in observed monthly runoff is generally well represented by the modelled runoff using climate simulations. However, monthly observed and modelled runoff show some disagreements. For example, in high-elevation catchments, the monthly runoff, generated using climate simulations, is generally underestimated in spring and early summer, whereas it is overestimated in late summer (Fig. 6; Fig. S16-17). This is likely to be related to the underestimation of temperature in these catchments in the climate simulations (Fig. 6).

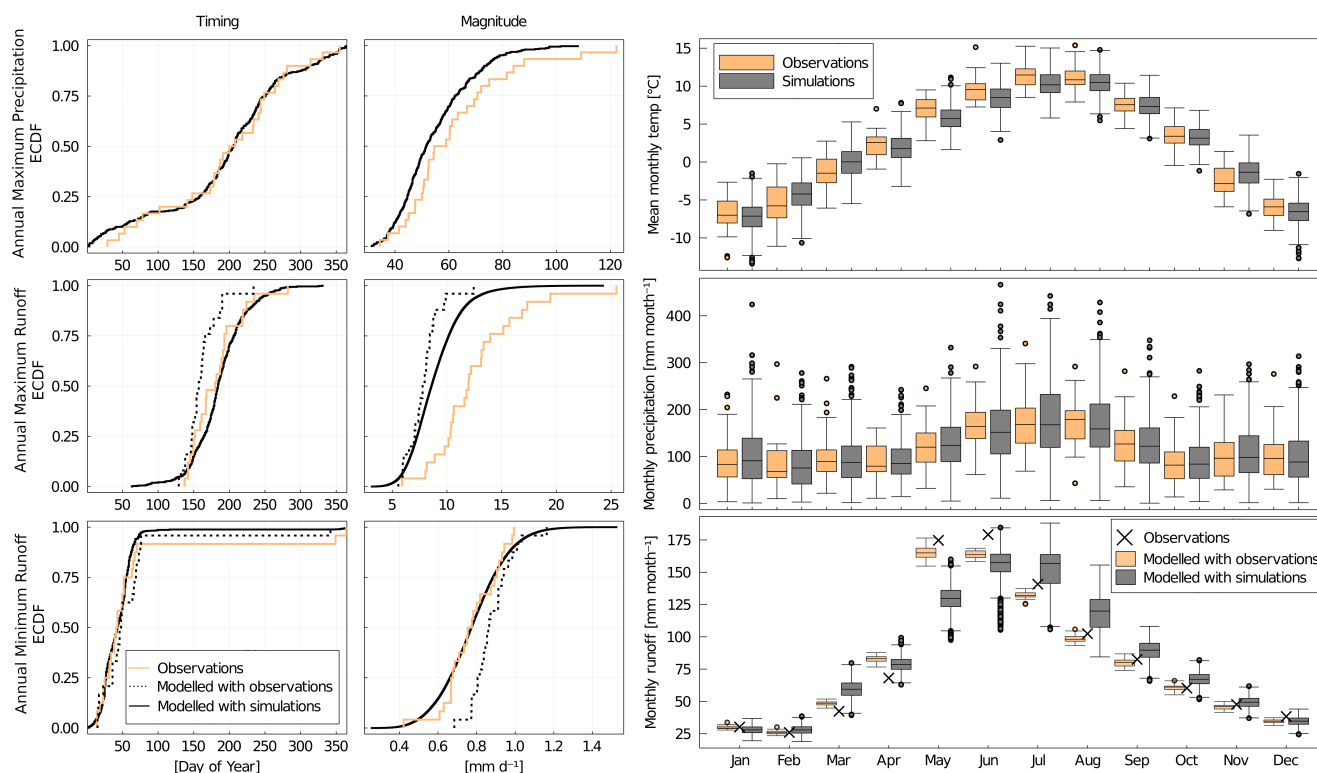


Figure 6. Comparison of past hydro-climatic data and runoff obtained from in situ observations and from climate simulations in the Silbertal catchment. The empirical cumulative distribution functions compare the timing and magnitudes of annual extremes derived from in situ observed data and from all climate models. The boxplots compare the distributions of mean monthly temperatures, monthly precipitation and monthly runoff derived from in situ observations and modelled climate. Note that the cross-symbols indicate the actual in situ observations of mean monthly runoff.

While the distributions of the timing of annual extreme events (e.g. the annual maximum precipitation, maximum runoff and minimum runoff), modelled under the simulated climate are broadly consistent with in situ observations, the distributions of the associated magnitudes of these annual extremes exhibit some more disagreement. Although, precipitation and minimum modelled runoff magnitudes obtained from in situ match those obtained from climate simulations generally well, observed annual maximum runoff is systematically underestimated by model results for all catchments (Fig. 6; Fig. S13-17). These underestimations are likely associated to an insufficient representation of localized, high-intensity rainfall events. As the main objective of the subsequent analysis is a quantification of the changes between the past and future flow characteristics rather than a prediction of absolute magnitudes, we assume, in the absence of more information, that these systematic errors remain constant over time and should therefore not significantly affect the interpretation of the analysis.

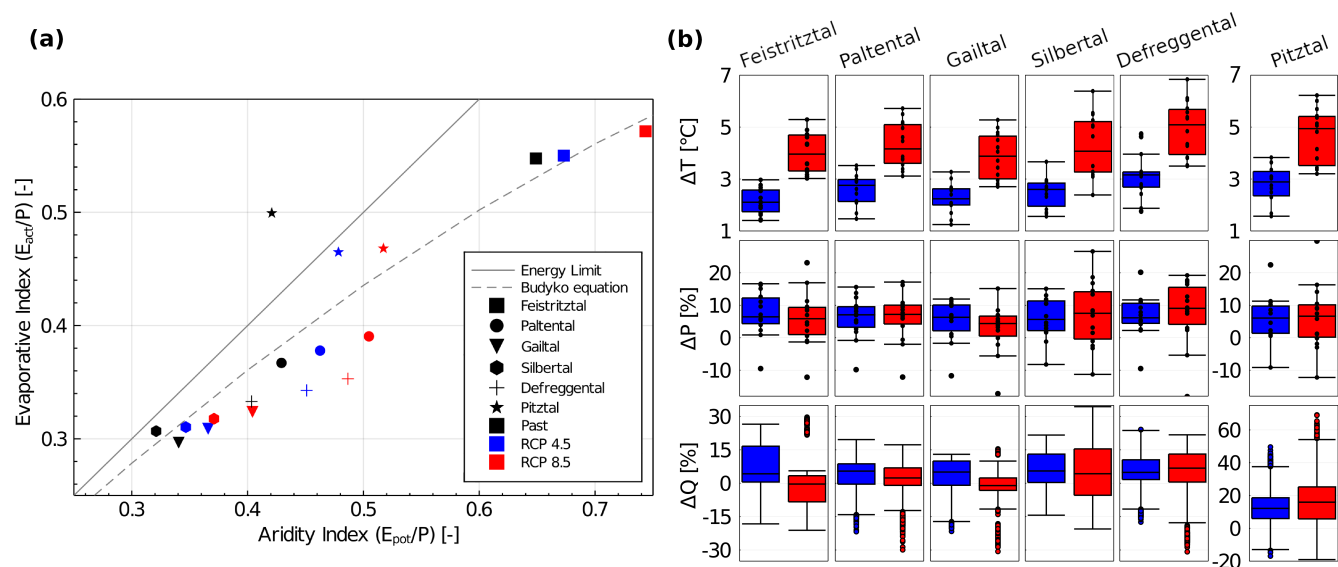


Figure 7. a) The position of the study catchments in the Budyko framework (Budyko, 1948) based on the 30-year means of all climate simulations in the past and under two emission scenarios at the end of the 21st century. E_{act} is actual evaporation defined as $1 - \frac{Q}{P}$; b) absolute changes between past and future in mean annual temperature as well as relative changes in mean annual precipitation of the 14 climate simulations (black dots representing the individual climate simulations) and in annual runoff of all simulations for RCP 4.5 (blue) and RCP 8.5 (red). Note the different scale for runoff of Pitztal.

3.3 Projection of future climate and hydrology

3.3.1 Annual, seasonal, and monthly averages

Firstly, the changes in average projected annual temperature, precipitation and modelled runoff between the 30-year periods in the past and the at the end of the 21st century are analyzed (Fig. 7b). The increase in temperature is similar across catchments, with a median increase across climate simulations of 2–3°C for RCP 4.5 and 4–5°C for RCP 8.5. On average, climate simulations show an increase of annual precipitation by 4% (RCP 8.5 Gailtal) to 9% (RCP 8.5 Defreggental). The median absolute change ranges from 50 mm yr⁻¹ to 100 mm yr⁻¹ across catchments. However, the spread between climate simulations is large, reaching from a decrease of 10% or larger for all catchments to an increase of more than 15%. Generally, a decrease in precipitation is projected for July and August for most catchments, while an increase in precipitation is projected for the rest of the year. For RCP 4.5, the modeled annual runoff exhibits an increase by around 5% for all catchments except the Pitztal, where a median increase of 12% was modelled (Fig. 7b). For RCP 8.5 the median change is around zero for the lower-elevation catchments Feistriztal, Paltental and Gailtal, whereas it is slightly larger than for RCP 4.5 in the Defreggental and Pitztal. Hence, the change in annual runoff is larger for high-elevation catchments under RCP 8.5. However, the spread between simulations is large.



240 Furthermore, the changes of the catchments in the Budyko framework follow a bottom-left to top-right trajectory, indicating
 a shift towards considerably more arid future conditions (Fig. 7a). Largely linked to increases in atmospheric water demand,
 i.e. Epot, this will lead to proportionally higher future evaporation and associated decreases in runoff coefficients. The change
 is around twice as large for the RCP 8.5 scenarios compared to RCP 4.5. Note that in the past, the Pitztal plots above the energy
 limit in the Budyko framework using modelled climate, but this is not the case when relying on in situ observed data. However,
 245 the impact on the results should be limited because a relative comparison of past and future runoff patterns is applied using
 climate simulations for both periods.

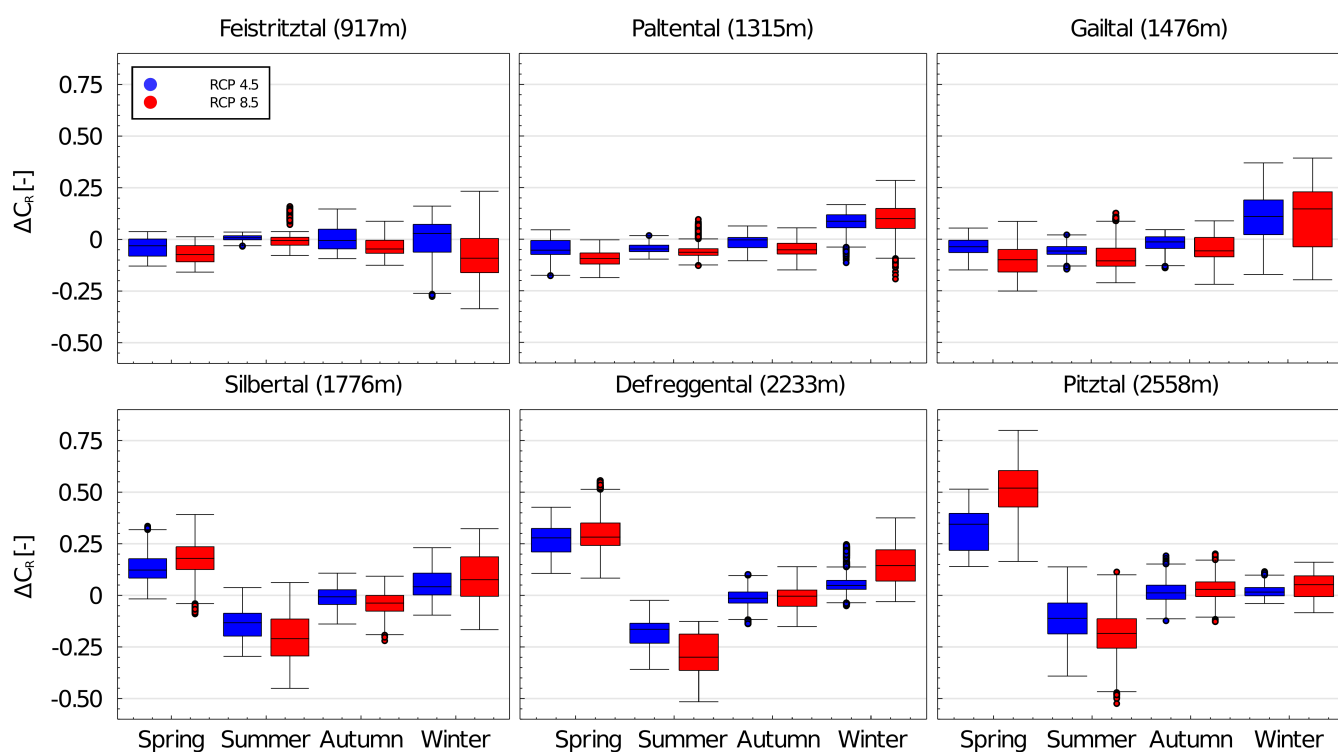


Figure 8. Absolute changes in mean seasonal runoff coefficient ($\Delta C_R [-]$); (spring: Mar–May, summer: Jun–Aug, autumn: Sep–Nov, winter: Dec–Feb) across all 14 simulations for the six study catchments and both scenarios RCP4.5 and RCP8.5. Mean catchment elevation is given in brackets.

Analyzing the change in seasonal modelled runoff coefficients $C_R = Q/P$, similarly reveals substantial differences between the low-elevation and the high-elevation catchments. For the high-elevation catchments, a median future increase in C_R across all 14 simulations is observed in spring ($\Delta C_R \sim 0.1$ – 0.5) and to a lesser extent in winter ($\Delta C_R < 0.1$) (Fig. 8), while the summer runoff coefficients experience considerable decreases by up to $\Delta C_R \sim -0.3$. In contrast, the lower-elevation catchments are mostly characterized by a decrease in median spring, summer and autumn runoff coefficients of up to $\Delta C_R \sim -0.1$ but an increase in winter ($\Delta C_R \sim 0.05$ – 0.15).

250

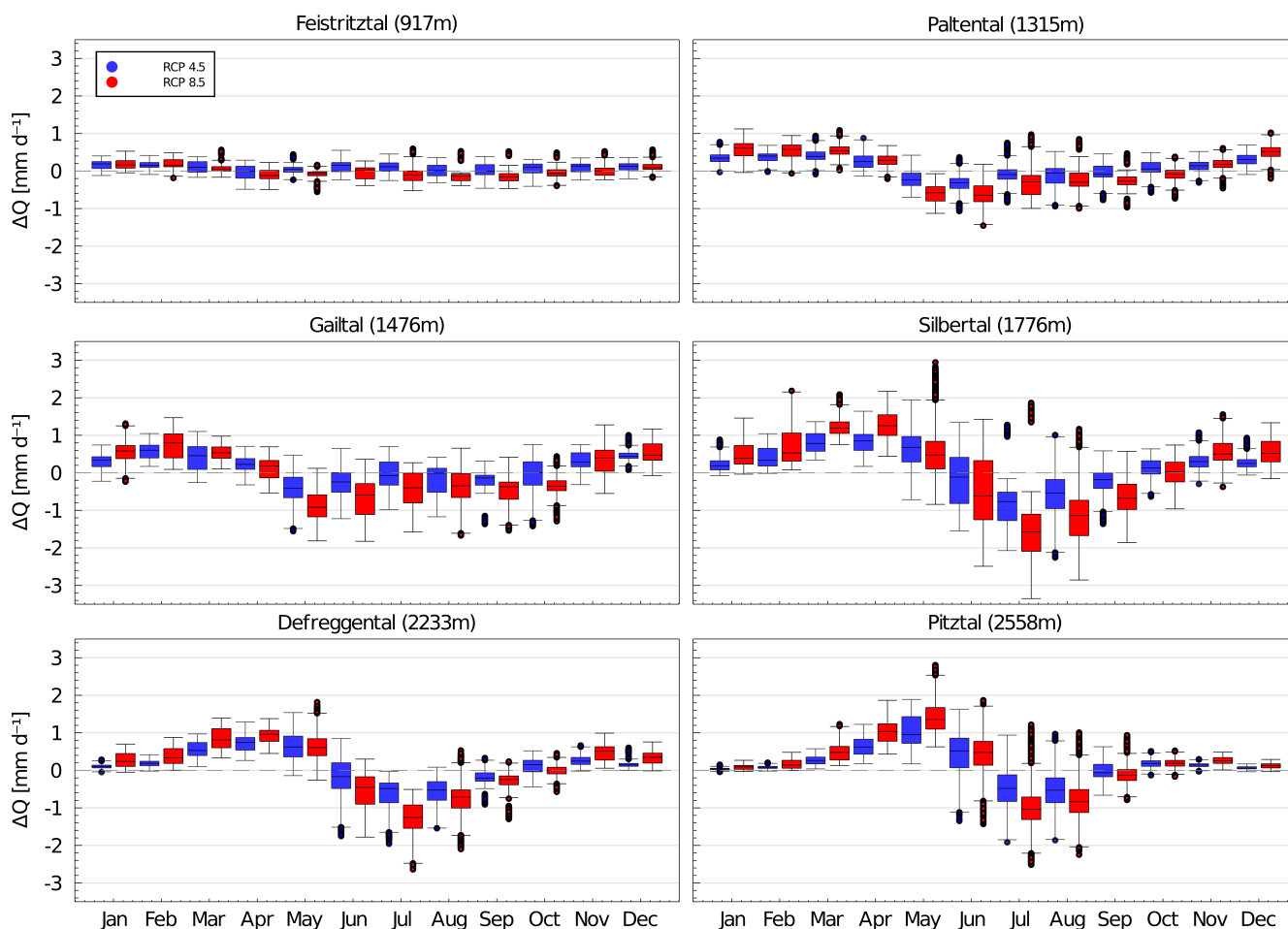


Figure 9. Absolute changes in future mean monthly runoff (ΔQ) across all simulations per RCP for the six study catchments. Mean catchment elevation is given in brackets

The modelled mean monthly runoff at the end of the century exhibits mostly consistent increases in winter and spring months ($\Delta Q \sim 25\text{--}100\%$ for RCP 4.5) and decreases in summer months ($\Delta Q \sim 10\text{--}20\%$ for RCP 4.5) in all study catchments (Fig. 255 9). Changes are up to twice as large for RCP 8.5 compared to RCP 4.5 and also the spread between simulations is larger. The largest relative and absolute increase in runoff occurs considerably later in high-elevation catchments. For the Gailtal catchment the largest absolute increase occurs in February ($\Delta Q \sim 0.6\text{--}0.8 \text{ mm d}^{-1}$), while for the Silbertal ($\Delta Q \sim 0.8\text{--}1.2 \text{ mm d}^{-1}$) and Defreggental catchments ($\Delta Q \sim 0.8\text{--}1.0 \text{ mm d}^{-1}$) this is the case in April and for the Pitztal catchment in May ($\Delta Q \sim 1\text{--}1.4 \text{ mm d}^{-1}$). The two lowest elevation catchments, i.e. Feistriztal and Paltental, do not show a distinct month with largest increase 260 in runoff. Decreases in monthly runoff can already be expected in May for the three low-elevation catchments, whereas this only occurs from June/July onwards in the high-elevation catchments (Fig. 9). The results also indicate that the magnitude of absolute change in monthly runoff generally increases with increasing mean catchment elevation. While the change is very



limited for the Feistritzal catchment ($\Delta Q \pm 0.2 \text{ mm d}^{-1}$), it is more pronounced in the Gailtal catchment ($\Delta Q \pm 0.9 \text{ mm d}^{-1}$), reaching the strongest decrease and increase in the Silbertal catchment ($\Delta Q \sim -1.5 \text{ mm d}^{-1}$) and Pitztal catchments ($\Delta Q \sim 1.5$ 265 mm d^{-1}), respectively.

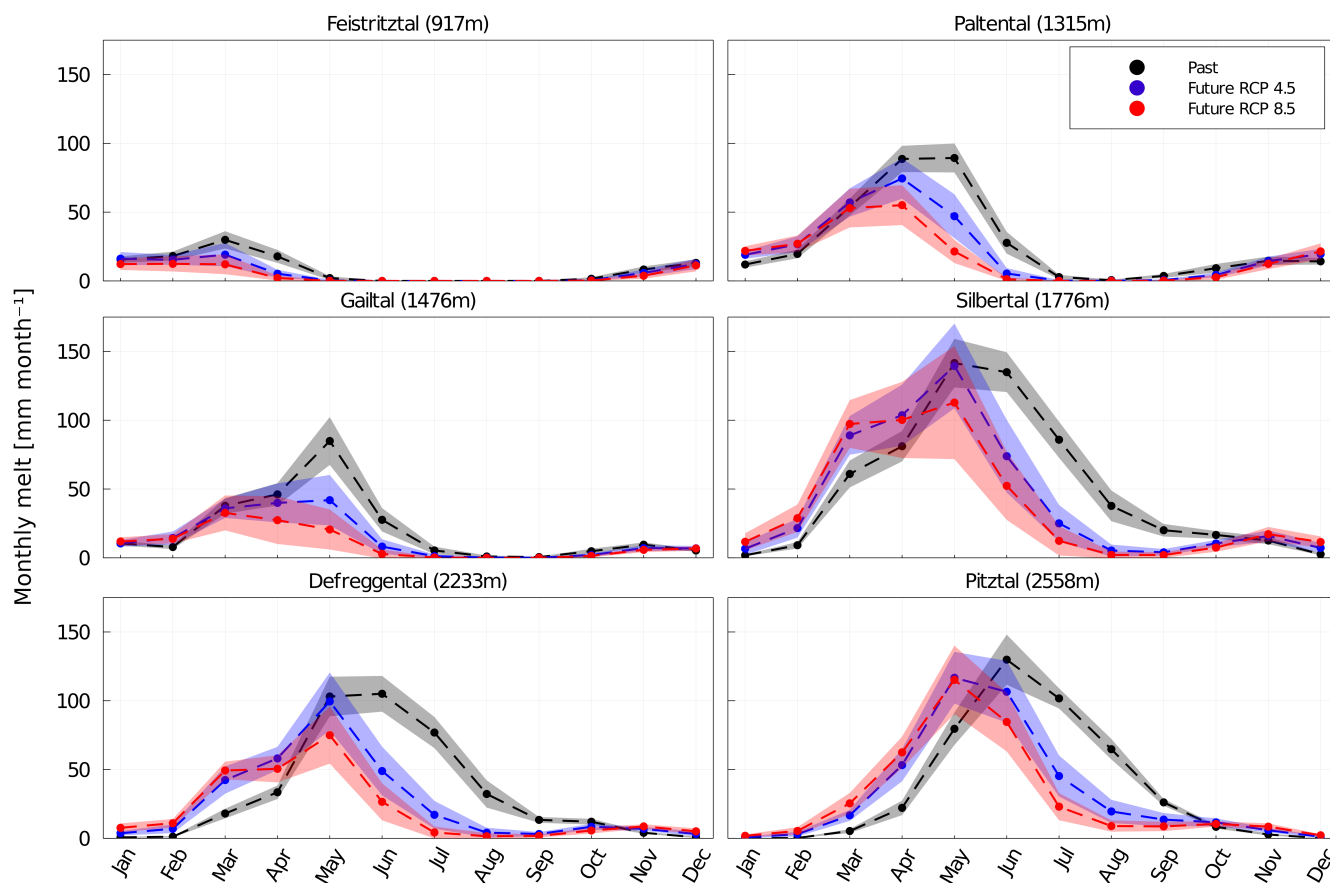


Figure 10. Mean monthly melt contributions in the past (black symbols) and future (blue symbols: RCP4.5, red symbols: RCP8.5) over the time period of 30-years. The shaded areas indicate the associated ± 1 standard deviations (grey: past, blue: RCP4.5 and red: RCP8.5). Dashed lines between the individual 15-day periods are used for better visualization

A decrease in future annual melt contribution is projected in all study catchments, ranging from $\Delta M \sim -10$ to -30% for RCP 4.5 and $\Delta M \sim -20$ to -55% for RCP 8.5. The results do not show the direct contribution of melt water to runoff but the contribution of melt water to the hydrological storages and processes that eventually generate runoff. The amount of melt water in the low-elevation Feistritzal catchment is small compared to all other catchments (Fig. 10). For the high-elevation 270 catchments, an earlier future onset of melt can be detected with a largest increase of $\Delta M \sim 25 \text{ mm month}^{-1}$ for the Silbertal and Defreggental catchments in March and $\Delta M \sim 35 \text{ mm month}^{-1}$ for the Pitztal in May. In addition, a remarkable decrease in melt from June through September is observed for the high-elevation catchments. Generally, the month with the largest melt



rates shifts to one month earlier in the year. Differences between the two emission scenarios are mostly visible in lower melt rates from May to July in most catchments for RCP 8.5. As opposed to the high-elevation catchments, no substantial increase in snow melt in the first months of the year is observed for the lower catchments.

Table 5. Mean and standard deviation of timing of annual maximum flow (AMF) across all simulations, based on the average timing of AMF over 30-years of each simulation. The dates are shown as day of year. For the past, the actual calendar date is given as reference.

	Past [d]	Date	RCP 4.5 [d]	RCP 8.5 [d]	Δt RCP 4.5 [d]	Δt RCP 8.5 [d]
Feistritzal	159±12	June 8	163±19	142±36	+4 days	-17 days
Paltental	165±9	June 14	163±17	151±23	-2 days	-14 days
Gailtal	277±25	October 4	306±22	325±21	+29 days	+48 days
Silbertal	186±8	July 5	166±12	155±17	-20 days	-31 days
Defreggental	188±9	July 7	177±13	179±17	-11 days	-9 days
Pitztal	185±7	July 4	171±11	163±15	-14 days	-22 days

3.3.2 Annual maxima (magnitude and timing)

A substantial shift in the timing of annual maximum flows (AMF) is observed towards the end of the 21st century, ranging on average from $\Delta t = -9$ to -31 days for high-elevation catchments and $\Delta t = +4$ to -17 days for low-elevation catchments (Table 5). More specifically, in the past, AMF occurred on average in the first week of July in the high-elevation catchments and around one month earlier in two of the low-elevation catchments (Feistritzal, Paltental). In the Gailtal catchment, AMF occurred on average in the first week of October. AMF in the higher catchments is characterized by a $\Delta t = -11$ to -20 days on average for RCP 4.5 with the Silbertal catchment exhibiting the largest shift of $\Delta t = -20$ days. For RCP 8.5, the Defreggental catchment shows a similar shift as for RCP 4.5, whereas the Silbertal and Pitztal catchments show an increased Δt of -31 and -22 days. The lowest catchments only exhibit a minor change in mean timing of AMF for RCP 4.5 and an average shift towards 2 week earlier occurrences for RCP 8.5. The Gailtal is the only catchment exhibiting a systematic and substantial shift towards later occurrences of AMF with a modelled mean $\Delta t = +29$ days for RCP 4.5 and $+48$ days for RCP 8.5. In addition, for all catchments except the Gailtal, the future standard deviation of the AMF timing increases (Table 5). However, mean timing may conceal bimodal distributions in timing of AMF. Analyzing the fraction of timing of occurrence within the individual 30-year time periods gives additional information about the intensity of seasonality (Fig. 11).

This analysis reveals a bimodal AMF distribution in the Gailtal catchment, with AMF potentially occurring in beginning of May or beginning of October. A relationship between mean elevation of the catchment and timing and seasonality of AMF can be observed for the past. For the lowest elevation catchment (Feistritzal), AMF occurrences are widely spread over the year with most occurrences around the beginning of May. The Paltental catchment shows most occurrences towards end of May, whereas the high-elevation catchments exhibit most AMFs in June and July and feature the highest seasonality. A systematic and significant shift towards earlier occurrences of annual maximum flows can be distinguished for the higher-elevation catchments. However, the model results suggest that also the Paltental catchment may experience a substantial future

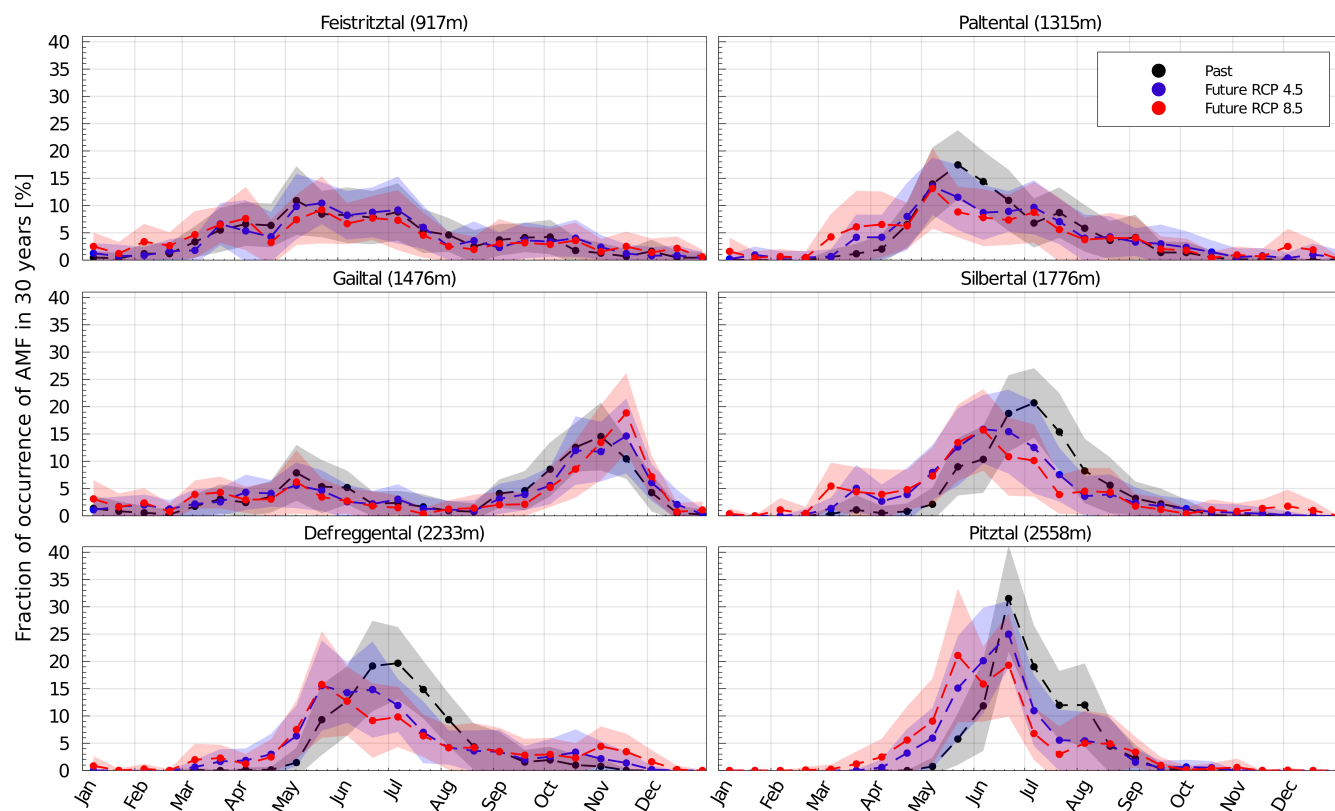


Figure 11. Mean fraction of occurrences of AMF in past (black symbols) and future (blue symbols: RCP4.5, red symbols: RCP8.5) for 30-year time periods using time windows of 15 days across all model simulations. The shaded areas indicate the associated ± 1 standard deviation. Dashed lines between the individual 15-day periods are used for better visualization.

increase in AMF occurrences in March for RCP 8.5. Across all study catchments, except the Gailtal catchment, the seasonality in timing of AMF is less pronounced in future. An extension of the potential future flood season by one to three months can be derived from visual inspection of Fig. 11. Changes are more pronounced for RCP 8.5 with a larger spread of timing of AMF over the year.

The change in modelled median average magnitude of AMF over 30-years (ΔAMF) is positive for all catchments under RCP 4.5 by $\sim 10\%$. The Paltental and Pitztal catchments show somewhat lower ($\Delta AMF \sim 2\%$) and higher increases ($\Delta AMF \sim 18\%$), respectively (Fig. 12a). The absolute changes are largest for the Gailtal ($\Delta AMF \sim 1.4 \text{ mm d}^{-1}$) and the Pitztal ($\Delta AMF \sim 1.1 \text{ mm d}^{-1}$). The ΔAMF is less pronounced in most catchments for RCP 8.5, even suggesting potential decreases of future AMF magnitudes in the Paltental catchment. However, the ranges of change and thus the uncertainties are large, in particular for the Paltental, Silbertal and Defreggental catchments, where simulations also indicate the possibility of a decrease in future AMF magnitudes. A larger absolute increase in magnitude of AMF for higher return periods is simulated as well as increasing uncertainty (Fig. 12b). The standard deviation of an ΔAMF associated with a return period of one year is 0.5 to 2 mm d^{-1} ,

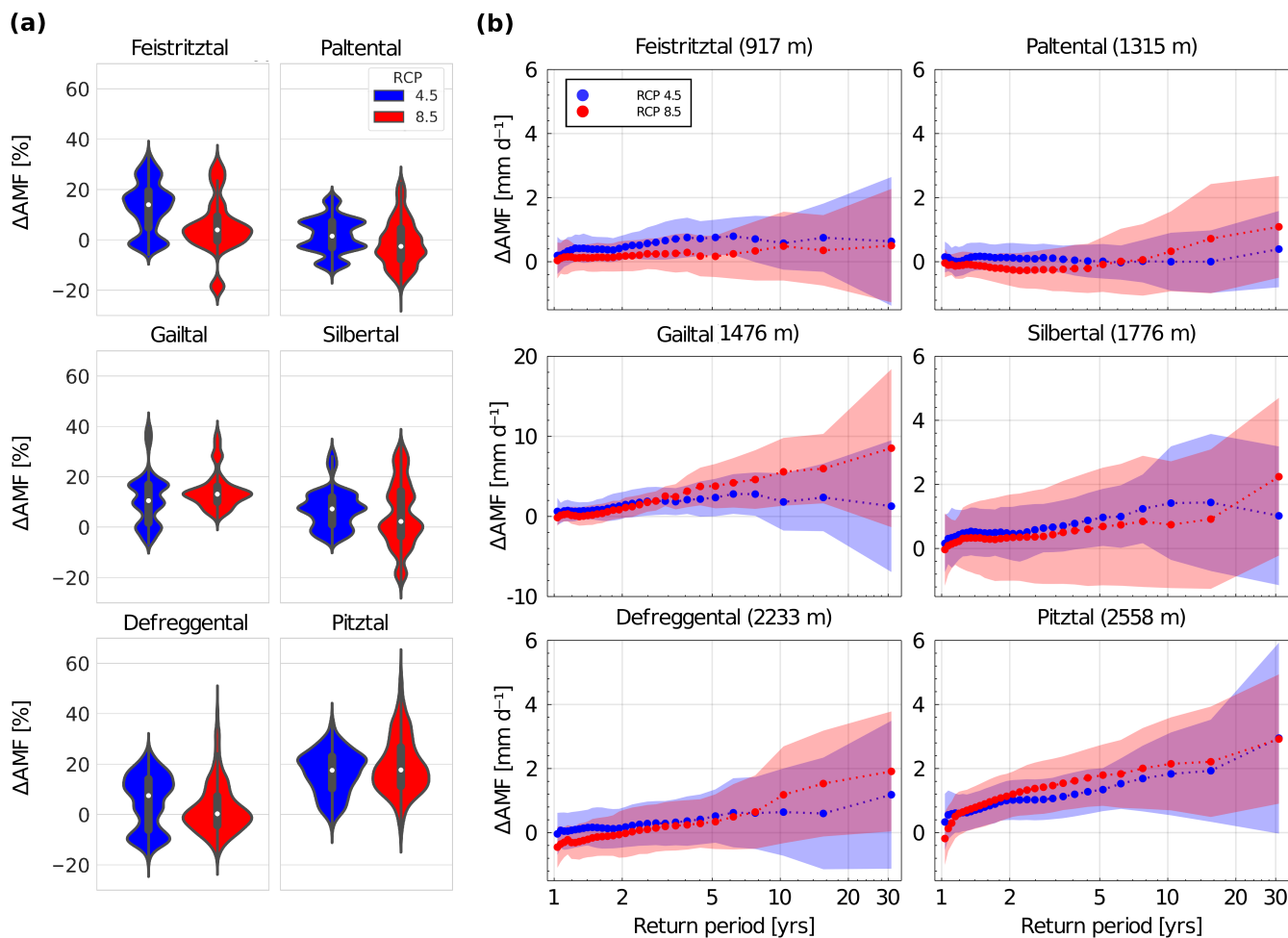


Figure 12. a) Violin plots of the relative change of magnitude of AMF across simulations based on average magnitude over 30-year time period of each simulation. b) Simulation mean absolute change in magnitudes of AMF in relation to the return period. Shaded area indicates 1 standard deviation, dotted lines are used for better visualization. Note the different scale for the Gailtal.

whereas it reaches 1.7–9 $mm\ d^{-1}$ for an ΔAMF associated with a return period of 30-years. A similar pattern can be observed
 310 for relative changes. The largest increase in magnitude of AMF at high return periods is found for the Gailtal for RCP 8.5
 with $\Delta AMF \sim 8\ mm\ d^{-1}$ (+40%), followed by the Pitztal with $\Delta AMF \sim 3\ mm\ d^{-1}$ (+32%) for both emission scenarios. The
 two lowest elevation catchments, Feistritzal and Paltental, only show smaller increases of $\Delta AMF \sim 0.6\ mm\ d^{-1}$ and $1.0\ mm\ d^{-1}$,
 respectively. For shorter return periods, the changes in ΔAMF are less pronounced and consistent across all catchments.

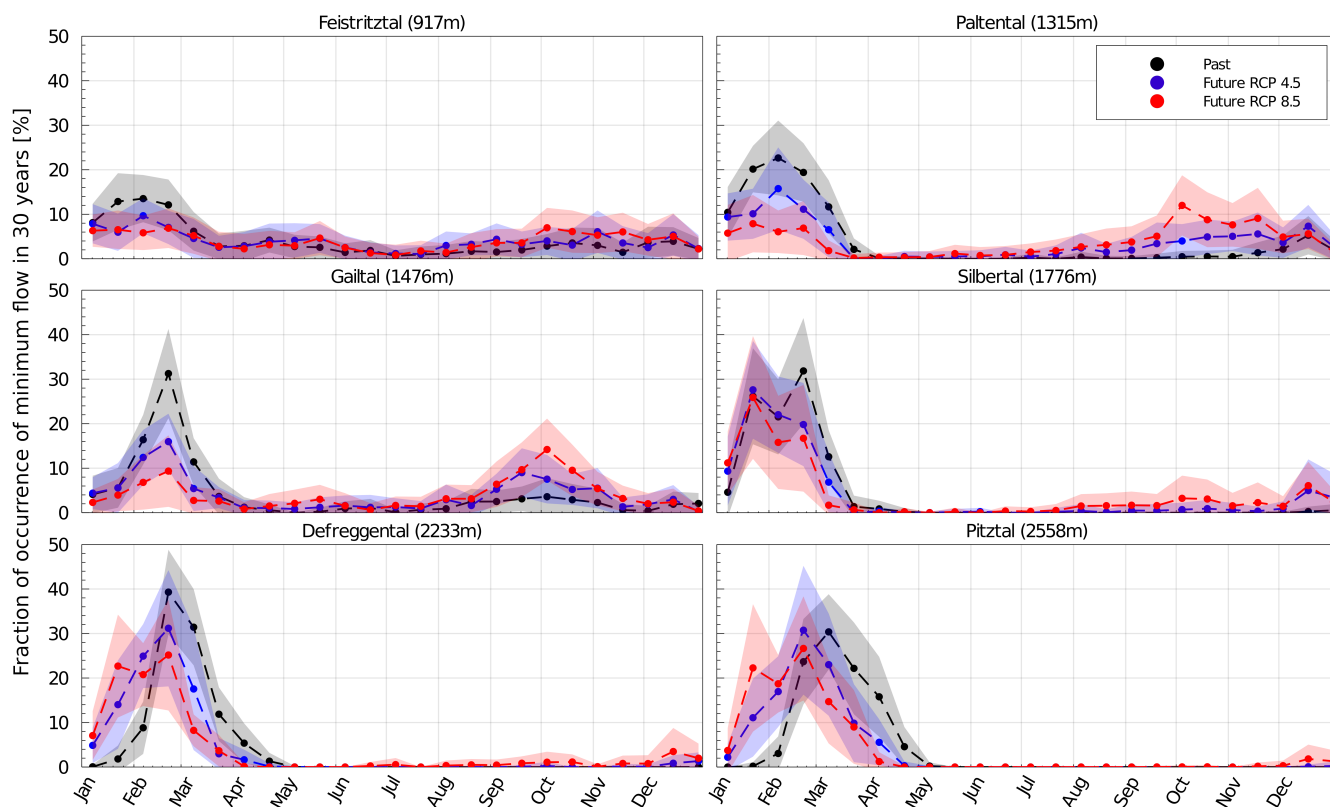


Figure 13. Mean fraction of occurrences of lowest annual 7-day flow in past (black symbols) and future (blue symbols: RCP4.5, red symbols: RCP8.5) 30-year time periods using time windows of 15 days across all model simulations. The shaded areas indicate the associated ± 1 standard deviation. Dashed lines between the individual 15-day periods are used for better visualization.

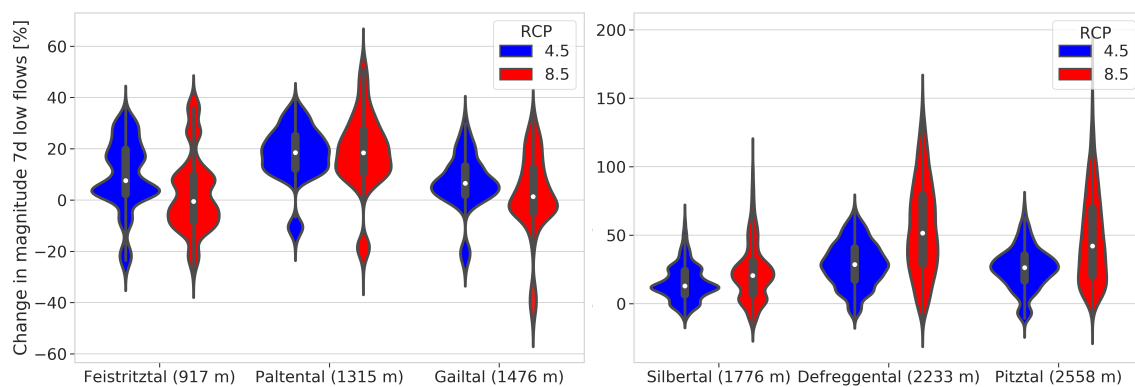


Figure 14. Relative change in magnitude of annual minimum 7-day flows for the late 21st century (2071–2100 vs. 1981–2100). Note the different scales for low- and high-elevation catchments.



3.3.3 Annual minima (magnitude and timing)

315 In line with observations, the modelled annual minimum flows in the past occurred mostly during the winter months in all study catchments. The model results suggest that for the low-elevation catchments, the fraction of occurrence of minimum flows in winter months decreases significantly in the future (Fig. 13). In particular, for RCP 8.5 the annual minimum flows shift towards early autumn, with around 13% of annual minimum flows occurring in late September in the Paltental and Gailtal catchments. In the lower-lying Feistritzal catchment, no clear seasonality in occurrence of minimum flows is distinguishable by the end
320 of the century. In the high-elevation catchments, past annual minimum flows occurred predominantly between late February to March. According to the model results, future annual minimum flows will occur earlier in the year, between January and February.

The magnitudes of the annual minimum flows show a remarkable potential median increase of 12–50% in the high-elevation catchments, with significantly larger increases for RCP 8.5 (Fig. 14). The high-elevation catchment Defreggental shows the
325 largest relative change with a median increase of 30/50% for RCP 4.5/8.5, while the second largest increase is simulated in the highest elevation catchment Pitztal with a median increase of 27/40% for RCP 4.5/8.5. Regarding the low-elevation catchments, the Paltental shows an increase in magnitude of minimum flows of 20% for both emission scenarios. The median increase in magnitude for the Feistritzal and Gailtal is below 10% for RCP 4.5 and around zero for RCP 8.5. While the Defreggental and Pitztal catchments may experience the largest relative median increases of up to 30/50% for RCP 4.5/8.5, the annual minimum
330 flows will be affected less in low-elevation catchments with median increases of up to around 20% for both emission scenarios. The absolute changes are largest for Paltental (+0.7 mm d⁻¹), followed by Defreggental under RCP 8.5 (+0.47 mm d⁻¹) and Gailtal catchments under RCP 4.5 (+0.35 mm d⁻¹). However, from the distributions around the medians (Fig. 14) it can also be seen that while increases in minimum flow are rather likely for the higher-elevation catchments, the direction of change is subject to much more uncertainty in the lower-elevation catchments.

335 4 Discussion

4.1 Changes in annual and seasonal climate and hydrology

For temperatures, the sign and magnitude of change are more consistent over all climate simulations than for precipitation. This corroborates the findings of previous climate impact studies in the region (e.g. Goler et al., 2016; Hanzer et al., 2018). The increase in projected future precipitation compared to the past is in contrast to other climate projections for Austria used
340 in previous studies, which suggested a decrease in precipitation (Stanzel and Nachtnebel, 2010). In addition, the modelled increase in annual runoff for the late 21st century (Fig. 6b) is not in line with results from other alpine catchments, which indicate no change or even a decrease in annual runoff (Goler et al., 2016; Muelchi et al., 2020). The median increase in annual runoff of around 5% for the study catchments under RCP 4.5 can be largely explained by the projected future precipitation increase of around 6%. Under RCP 8.5, the low-elevation catchments show a median change in annual runoff of $\Delta Q \sim -1.5$ to
345 2%, which is much lower than the precipitation increase of $\Delta P \sim 4.5$ -7%. This slightly lower annual runoff can be attributed to



changes in the future partitioning of water fluxes and thus an increased fraction of precipitation to be evaporated (cf. Fig. 6a). This general decrease in mean runoff coefficients in a warmer climate strongly supports earlier studies (e.g. Berghuijs et al., 2014). The results further strongly suggest that changes in seasonal runoff coefficients and melt contributions are related (Fig. 8 & 10). In seasons with decreasing future melt contributions (i.e. spring/summer for low-/high-elevation catchments), the runoff coefficient decreases, whereas it increases in spring for high-elevation catchments, where melt contributions increase in the future. This implies that changes in snow contributions are more important for changes in seasonal runoff than changes in precipitation, as precipitation is projected to increase in future winter and spring seasons. The decrease in summer and autumn runoff coefficients can be explained by decreased precipitation and increased evaporation, which is evident in low-elevation catchments by an increased number of minimum flow events in autumn (Fig. 13).

355 4.2 Changes in monthly runoff

The modelled changes in monthly runoff correspond well with the results of previous studies in the region (Stanzel and Nachtnebel, 2010; Laghari et al., 2012; Tecklenburg et al., 2012), which also report an increase in winter and spring runoff and a decrease in summer runoff. The largest increase in winter runoff occurs later in the season for the high-elevation catchments, which supports findings by Stanzel and Nachtnebel (2010). An explanation gives the later onset of the melting season by one month or more in high-elevation catchments (Fig. 10), resulting in increased runoff in later months compared to the low-elevation catchments. Hanzer et al. (2018) simulated changes in monthly runoff in the upper part of the Pitztal and found largest increases in March of around 80% (150%) for RCP 4.5 (RCP 8.5) and largest decreases in August of around 50%, which is close to results of this study, with increases of around 100 to 180% in March, and decreases in August of 20 to 40% (Fig. 9).

The increases in future winter runoff can be related to an increase in precipitation (December to February), while increases in melt contribution are largely responsible for the increase in future spring runoff (March to May). In the first two months of the year with negative changes in monthly runoff, the decrease of $\Delta Q = -5$ to -24 mm month⁻¹ can be attributed to a decrease in melt contribution ($\Delta M = -18$ to -56 mm month⁻¹) in combination with increased potential evaporation ($\Delta E_{\text{pot}} = 5$ - 12 mm month⁻¹). Conversely, future precipitation still increases in these months ($\Delta P = 1$ - 24 mm month⁻¹). However, the future decreases in runoff during late summer in the low-elevation catchments ($\Delta Q = -3$ to -5 mm month⁻¹) are mainly a consequence of decreased summer precipitation ($\Delta P = -4$ to -8 mm month⁻¹) in combination with increased potential evaporation ($\Delta E_{\text{pot}} = 7$ - 9 mm month⁻¹) as melt contributions become negligible.

The higher importance of melt contribution for summer runoff in high-elevation catchments compared to the low-elevation catchments can also explain the larger decrease in summer runoff of $\Delta Q = -14$ to -24 mm month⁻¹ compared to $\Delta Q = -6$ to 13 mm month⁻¹ in the low-elevation catchments. Furthermore, a decrease in melt contribution from glaciated areas could potentially be of importance for the decrease in summer runoff in the Pitztal (Hanzer et al., 2018; Laurent et al., 2020). Overall, the decrease in melt contribution and increase in potential evaporation influence the change in monthly runoff more than the changing precipitation patterns, as the maximum decrease in monthly runoff occurs earlier than for monthly precipitation.

The decrease in summer runoff under RCP 8.5 is more pronounced than for RCP 4.5. This can be explained by a stronger decrease in melt contribution, an increased evaporation and a mostly stronger decrease in monthly precipitation under RCP



380 8.5. The winter and spring runoff under RCP 8.5 show an additional increase of $\Delta Q = 2$ to 14 mm month^{-1} compared to RCP
4.5, resulting from a larger increase in snow melt (Fig. 10). This increased snow melt directly relates to higher temperatures,
as well as a larger average increase in precipitation in winter months under RCP 8.5. The Feistritzal is the only catchment
with a similar modelled median increase in winter runoff for both emission scenarios. A possible explanation is that the larger
decrease in snow contribution is balanced by the higher precipitation under RCP 8.5, resulting in a similar change in runoff
385 under both emission scenarios.

4.3 Annual maxima (magnitude and timing)

The mean timing of AMF in October for the Gailtal, as well as June and July for the other catchments, in the past supports
the findings of previous studies (Parajka et al., 2009; Blöschl et al., 2011). The high-elevation catchments show a high flood
seasonality in the past, suggesting snow melt as a dominant flood-generating process. For the future, earlier snow melt is then
390 likely to result in significant shifts in the timing of AMF towards earlier occurrences ($\Delta t \sim -9$ to -31 days). For the late 21st
century, AMF occur mostly in May and in the beginning of June as compared to mid-June to early July in the past, which
corresponds well with the expected future shift in timing of maximum monthly melt contributions from June to May. Parajka
et al. (2010) identified snow melt and rainfall as important flood generation mechanism in the central Alps. A change in flood-
generating processes from snow melt to precipitation in mountainous catchments and thus a shift in flood season towards
395 season with highest precipitation was observed in other studies by Vormoor et al. (2015) and Brunner et al. (2020). Thus,
changes in precipitation patterns are also likely to contribute to the change in timing of AMF as June and July were the months
with highest precipitation in past but future precipitation increases are most pronounced in June.

The autumn nival flow regime of the Gailtal is characterized by maximum flows in late spring due to snow melt and a
secondary maximum of flow in autumn due to intensive precipitation (Mader et al., 1996), which translates into high flows
400 occurring both in late spring and autumn (Blöschl et al., 2011). The significant future shift towards later occurrences in AMF
in the Gailtal, on the one hand, can be mostly attributed to changes in precipitation patterns, with a larger increase in precipita-
tion in November as compared to October (particularly under RCP 8.5), as the timing of floods in southern Austria is strongly
influenced by Meridional south-east and south weather regimes (Parajka et al., 2010). On the other hand, earlier annual maxi-
mum flows are generated during the first half of the year related to the combination of earlier snow melt and increased spring
405 precipitation. The average shift of half a month towards earlier occurrences of AMF in the low-lying Feistritzal and Paltental
for RCP 8.5 is likely related to a more pronounced decrease in AMF occurrences in the summer months. The latter is linked to
increased evaporation, and a larger increase in occurrences in spring and winter compared to RCP 4.5, connected to increased
winter precipitation.

The shift towards later AMF occurrences in the Gailtal catchment and earlier AMF occurrences in the other catchments
410 supports projections for Alpine regions in Switzerland, although no shift in AMF seasonality of highly glaciated catchments
was projected there (Muelchi et al., 2021). The seasonality of AMF decreases in the future and the potential flood season
expands by up to three months, which is also suggested by Dobler et al. (2012), Köplin et al. (2014) and Schneeberger et al.
(2015). This indicates that future AMF is not only generated by snow melt or the combination of snow melt and precipitation



but more often only by precipitation. In summary, the timing of AMF in high-elevation catchments with nival flow regimes will
415 continue to largely depend on snow melt. This emphasizes the importance of temperature change for runoff patterns in alpine
catchments. In contrast, in the low-elevation catchments, where a seasonality in timing of AMF is less pronounced today, future
shifts occur mostly due to changes in precipitation patterns and increased evaporation.

The mean increase in magnitude of AMF for all catchments, except for the Paltental for RCP 4.5, is in contrast to findings
by Holzmann et al. (2010) who reported a future decrease in AMF magnitudes for meso-scale catchments in Western Austria.
420 Similarly, the results of Thober et al. (2018) suggest a decrease in maximum runoff for the Alps under future climate conditions.
However, for Swiss catchments a future increase in AMF magnitude was projected by Köplin et al. (2014), whereas results of
Muelchi et al. (2021) indicate a slight decrease in AMF magnitudes in Swiss catchments and Brunner et al. (2019a) expect a
future decrease or no change in maximum runoff under extreme flow regimes in melt-dominated areas in Switzerland. In this
study, a similar relative mean modelled AMF increase in all catchments was modelled for RCP 4.5 ($\Delta Q \sim 10\%$), suggesting
425 increased precipitation as the underlying reason, since monthly precipitation increases for all catchments during the main flood
season (6 to 15%) and precipitation intensity rises by 5 to 18%. As the dominant generating mechanism shifts from snow melt
towards rain, increases in AMF magnitudes are possible because they are no longer limited by the amount of snow storage
available for melt (Merz and Blöschl, 2003). This is also supported by findings of Schneeberger et al. (2015) for the Lech
catchment in Austria, where an increase in temperature without changes in precipitation only leads to minor shifts in flood
430 intensities. The low median increase in AMF magnitude in the Paltental of $\Delta Q \sim 2\%$ under RCP 4.5 with large uncertainties
is largely the consequence of the strong decrease in snow melt contribution in May and June, which offsets increases in
precipitation and maximum precipitation intensity.

Interestingly, the increase in mean AMF magnitude is lower for four out of six catchments under RCP 8.5 compared to
RCP 4.5. This indicates that not all changes in runoff patterns are more pronounced for the higher emission scenario. In the
435 lowest-elevation catchments, Feistritztal and Paltental, increased precipitation is offset by a >50% larger increase of potential
evaporation under RCP 8.5. This results in larger dry season soil storage deficits, which buffer precipitation and thereby moderate
annual maximum flows. For the high-elevation catchments, Defreggental and Silbertal, snow contribution is important
in the generation of annual maximum flows. Under RCP 8.5 the largest monthly melt contribution, which occurs in May, is
lower than under RCP 4.5, for which monthly melt contribution was similar for the late 21st century compared to today (see
440 Fig. 10). This decrease in melt contribution, together with higher potential evaporation, is more important for change in AMF
magnitudes than the increase in precipitation intensities of 14–20% for RCP 8.5 compared to 5–16% for RCP 4.5. In the Pitztal,
the maximum monthly melt contribution remains similar under both emission scenarios, which can be an explanation for the
similar increase in AMF magnitude. Overall, the changes induced by increased temperature have a larger effect on the changes
in AMF magnitudes under RCP 8.5 than changes in precipitation. The latter, however, remain the dominant control on AMF
445 magnitude increases under RCP 4.5.

The increase in AMF magnitude is larger for high return periods, especially under RCP 8.5. This is a likely consequence
of the higher increase in extreme precipitation intensities compared to mean precipitation intensities. However, also the un-
certainty in AMF magnitudes at higher return periods increases. The increase in runoff for a 30-year return period modelled



in this study is much larger ($\sim 40\%$ for RCP 8.5) than the increase in runoff for a 100-year return period (HQ100) of 4% for
450 the Gailtal for the mid of the 21st century suggested by Blöschl et al. (2011). For catchments in the region of Silbertal, De-
freggental and Pitztal, the study by Blöschl et al. (2011) suggests a decrease in HQ100, which contrasts with our model results.
For this comparison, it should be noted that a large uncertainty surrounds runoff magnitudes of high return periods (Fig. 12).
One reason for the pronounced uncertainties relates to the evaluation of extreme events, which strongly depends on the chosen
time period. Other studies conclude that the natural variability in magnitude of high flows exceeds the change due to climate
455 change, which particularly increases uncertainty for high return periods (Blöschl et al., 2011; Dobler et al., 2012).

4.4 Annual minima (magnitude and timing)

In the higher alpine catchments, the modelled shift towards earlier occurrences of low flows to January and February can be
explained by an increase in melt contributions in February to April that translates into an increase in monthly runoff. The
minimum flows occur before melting starts. In the low-elevation catchments, the shift in timing of minimum flows from winter
460 to autumn is mostly linked to an increased potential evaporation (particularly pronounced in July) as well as mostly decreasing
monthly precipitation in July to September. Thus, an increased storage deficit in the unsaturated zone in late summer due to
increased evaporation leads to longer storage of precipitation before it is released as runoff. This is also reflected by decreased
seasonal runoff coefficients in summer and autumn (Fig. 8). The reduction of the monthly water deficit in winter and an
increase in late summer projected in this study, is in line with findings by Goler et al. (2016) for other Austrian catchments,
465 who predict a reduction of days below the Q_{95} threshold in winter but an increase in summer. Projections of minimum flows
in Switzerland indicate timing predominately between August and October (Muelchi et al., 2021), whereas our results indicate
future occurrences of minimum annual flows, both, in winter and autumn.

The magnitude of the annual minimum runoff mostly increases in high-elevation catchments by $\Delta Q \sim 12\text{--}50\%$, which can
be related to higher winter precipitation and decreased amount of water stored as snow (Laaha et al., 2016; Parajka et al., 2016;
470 Marx et al., 2018; Brunner et al., 2019a; Muelchi et al., 2021). Whereas projections for lower catchments in Switzerland show
an apparent future decrease in magnitude of minimum annual flows for RCP 8.5 (Muelchi et al., 2021), our projections show
uncertainty in the sign of change.

4.5 Societal impacts

Changes in monthly runoff impact seasonal water availability. In the future, there will be more water available in winter and
475 less in summer across the study region. This could lead to a mismatch between water supply and water demand as mountain
regions of the Alps are classified as supportive for the lowlands (Viviroli et al., 2007). However, the Alps are identified as
basins where present water demands can also be met in 2060 (Mankin et al., 2017). Therefore, water scarcity due to changes in
runoff dynamics in the Alps seems unlikely (Immerzeel et al., 2020). Changes in runoff also impact hydro-power production
(Schaeffli et al., 2019). This study found mostly an increase in annual runoff in future, which may have a positive impact on
480 hydro-power generation. Nevertheless, seasonal changes can lead to decreased energy production in summer and autumn and
increased energy production in winter and spring. Management schemes of hydro-power production may need to be adapted



to such changing seasonal water availabilities, which could potentially be realized by storing seasonal melt water in artificial basins (Farinotti et al., 2019). Adaptation measures are likely to be higher for RCP 8.5. With respect to annual maximum flows, an increase of magnitudes of maximum flows may locally entail the need to carefully review flood risk assessments and safety of hydraulic structures designed for lower flood estimates. In addition, the likely extension of the potential flood season will lead to less predictability in the timing of future flood events.

4.6 Climate model uncertainty

The results of individual climate models per RCP were compared to investigate whether a specific climate model (Table 2) corresponds to large systematic changes in the hydrological response across all study catchments. Generally, no single climate model was found to lead to largest or lowest changes across catchments or across emission scenarios. However, there are substantial differences in modelled changes between climate models. The model with largest decrease/increase in precipitation yielded largest/smallest decreases in monthly runoff in summer and early autumn. For changes in runoff in other months, no relationship between the most extreme changes and a given model was found. The climate model with strongest decrease in annual precipitation (model 10) produces the smallest changes in the magnitude of annual minimum and maximum flows, whereas the model with largest increase in annual precipitation mostly results in the largest increases in magnitudes. Regarding timing of AMF, the smallest/largest shift towards earlier occurrences is found for the climate models with the largest increase in precipitation/temperature under RCP 8.5. The relationship between climate model and timing of minimum flows is less clear. The results indicate that the employment of an ensemble of climate models is indispensable. Extremes in changes for different catchments and emission scenarios can often not be traced back to a single model. The single model resulting in most extreme changes across catchments is model 10 due a substantial decrease in precipitation.

4.7 Uncertainty & limitations

There are several sources uncertainty in the above analysis, which are mostly associated with input data and choices made during the modeling process. Besides observation errors, the point-scale precipitation data are likely not to be fully representative of the catchment-scale precipitation in the study catchments. This is in particular true for the occurrence of localized convective high-intensity summer rain storms (e.g. Hrachowitz and Weiler, 2011)). In addition, the complex terrain may cause spatially complex precipitation fields and elevation gradients that are not captured by the available data. This very likely also explains the mismatch of precipitation and runoff data in the Silbertal and Defregental, which is most obvious in the frequent underestimation of modelled peak runoff. Since runoff processes are nonlinear, systematic errors likely do change in the future, although the effect may be small, undermining the assumption that systematic errors will be constant over time. Therefore, results related to the magnitude of maximum runoff are less reliable, likely indicating the lower limits of change. Furthermore, during the implementation of the model, many choices had to be made regarding the representation of processes and specific parametrizations. Each decision was taken carefully but still encompasses uncertainties. For example, the choice of estimation method for potential evaporation influences the results and thus introduces uncertainty (Seiller and Anctil, 2016). Similarly, snow processes are simplified by using a degree-day method and, in the absence of more detailed data, not considering snow



515 redistribution and sublimation, although it can have a significant effect in high-elevation areas (MacDonald et al., 2010). An-
other uncertainty arises from calibrating the model with in situ observed data but using projection data for the future. To reduce
this limitation, data of the same spatial scale was used. Nevertheless, temperature of climate simulations underestimated the
measured temperatures in the past for high-elevation catchments. This is a likely explanation for the implausible position of
the Pitztal in the Budyko framework (Fig. 7), because lower temperatures lead to enhanced snow accumulation and decreased
520 runoff. Moreover, system characteristics and thus model parameters are assumed to remain constant over time because of
lack of knowledge regarding such potential changes. However, in reality parameters such as maximum storage capacity in the
unsaturated root zone can change due to for instance vegetation adaptation to changing climate. This limitation also applies
to most other studies investigating future climate change impacts (e.g. Laghari et al. (2012); Parajka et al. (2016); Marx et al.
(2018)). Another uncertainty for future changes in runoff patterns stems from land use change. Natural and human induced land
525 use change can alter hydrological responses significantly (Jaramillo and Destouni, 2014; Nijzink et al., 2016; Thielen et al.,
2016; Hrachowitz et al., 2020). Land use is incorporated in the model through different HRUs for bare, forested and grassland
hillslopes, which differ in parameters for landscape dependent processes (see Fig. 2). Land use change could be represented
by changing the areal extents of specific HRUs. Nonetheless owing to its large intrinsic uncertainty, land use change was not
considered in this study, except for glacier retreat.

530 One of the largest uncertainties in climate impact assessment – the utilized climate model – has been taken into account
in this study, which contrasts with previous studies focusing on the Austrian Alps, by using an ensemble of climate models.
Within this context, it is crucial to stress that all results of this study are conditional on the considered climate simulations.

5 Conclusions

The aim of this study was to investigate the effect of climate change on late 21st century runoff patterns, particularly annual
535 extremes, over a cross section of different elevations and landscapes in Austria using an ensemble of climate models. To get
a comprehensive view on these changes, various aspects of runoff were studied. The results provide evidence of significant
changes in future runoff patterns in alpine catchments due to climate change. Future changes were found to be more pronounced
for high-elevation catchments, due to the high dependence on snow dynamics.

For high-elevation catchments, a substantial shift was found in the timing of annual maximum flows to earlier occurrences
540 (up to a month), as well as an extension of the potential flood season by one to three months. For lower-elevation catchments,
shifts in timing are less clear. A mean increase in AMF magnitudes was determined with more pronounced changes for RCP
4.5 than for RCP 8.5. Another main finding of this study was the occurrence of a shift towards earlier annual minimum flows in
January and February in high-elevation catchments, whereas in lower-elevation catchments annual minimum flows shift from
the beginning of the calendar year to autumn. While all catchments showed an increase in magnitudes of minimum flows under
545 RCP 4.5, no change or decreases were found for two of the lower-elevation catchments under RCP 8.5.

The findings suggest a relationship between the elevation of catchments and changes in timing of annual maximum and
minimum flows and magnitude of low flows. In contrast no relationship between elevation and magnitude of annual maximum



flows could be distinguished. Future research should focus on modelling climate change under different land use change scenarios in alpine catchments to allow exploring the importance of land use change and identifying scenarios under which climate change impacts are intensified or weakened.

Code and data availability. Hydro-meteorological data were provided by Hydrological Service Austria and ZAMG. The climate simulation data was produced by Wegener Center for Climate and Global Change, University of Graz (Douglas Maraun, Matt Switanek). The model code is available via (<https://github.com/sarah-hanus/hbv-mountain>) or from the first author directly. The modelled runoff data generated in this study is available via <https://doi.org/10.5281/zenodo.4539986>.

Author contributions. SH developed the model code, performed the simulations, did the analysis and drafted the manuscript. MH designed the study. RK provided hydro-meteorological data. HZ provided glacier projection data. All the authors discussed the results and contributed to writing the final manuscript.

Competing interests. The authors declare that they have no conflict of interest.

Acknowledgements. We would like to thank Dr. Matt Switanek, who generated the climate simulations and made them available for this study. Harry Zekollari acknowledges the funding received from a EU Horizon 2020 Marie Skłodowska-Curie Individual Fellowship (Grant 799904).



References

- Abermann, J., Fischer, A., Lambrecht, A., and Geist, T.: On the potential of very high-resolution repeat DEMs in glacial and periglacial environments, *The Cryosphere*, 4, 53–65, <https://doi.org/10.5194/tc-4-53-2010>, 2010.
- 565 Addor, N., Rössler, O., Köplin, N., Huss, M., Weingartner, R., and Seibert, J.: Robust changes and sources of uncertainty in the projected hydrological regimes of Swiss catchments, *Water Resources Research*, 50, 7541–7562, <https://doi.org/10.1002/2014WR015549>, 2014, 2014.
- Barnett, T. P., Adam, J. C., and Lettenmaier, D. P.: Potential impacts of a warming climate on water availability in snow-dominated regions, *Nature*, 438, 303–309, <https://doi.org/10.1038/nature04141>, 2005.
- 570 Bavay, M., Grünewald, T., and Lehning, M.: Response of snow cover and runoff to climate change in high Alpine catchments of Eastern Switzerland, *Advances in Water Resources*, 55, 4–16, <https://doi.org/10.1016/j.advwatres.2012.12.009>, 2013.
- Berghuijs, W., Woods, R., and Hrachowitz, M.: A precipitation shift from snow towards rain leads to a decrease in streamflow, *Nature Climate Change*, 4, 583–586, <https://doi.org/10.1038/nclimate2246>, 2014.
- Beven, K. and Binley, A.: The future of distributed models: model calibration and uncertainty prediction, *Hydrological Processes*, 6, 279–298, 575 1992.
- Blöschl, G., Viglione, A., Merz, R., Parajka, J., Salinas, J., and Schöner, W.: Auswirkungen des Klimawandels auf Hochwasser und Niedrigwasser, *Österreichische Wasser- und Abfallwirtschaft*, 63, 21–30, 2011.
- Blöschl, G., Hall, J., Parajka, J., Perdigão, R. A., Merz, B., Arheimer, B., Aronica, G. T., Bilibashi, A., Bonacci, O., Borga, M., et al.: Changing climate shifts timing of European floods, *Science*, 357, 588–590, <https://doi.org/10.1126/science.aan2506>, 2017.
- 580 Blöschl, G., Hall, J., Viglione, A., Perdigão, R. A., Parajka, J., Merz, B., Lun, D., Arheimer, B., Aronica, G. T., Bilibashi, A., et al.: Changing climate both increases and decreases European river floods, *Nature*, 573, 108–111, <https://doi.org/10.1038/s41586-019-1495-6>, 2019.
- Brunetti, M., Lentini, G., Maugeri, M., Nanni, T., Auer, I., Boehm, R., and Schoener, W.: Climate variability and change in the Greater Alpine Region over the last two centuries based on multi-variable analysis, *International Journal of Climatology: A Journal of the Royal Meteorological Society*, 29, 2197–2225, <https://doi.org/10.1002/joc>, 2009.
- 585 Brunner, M. I., Farinotti, D., Zekollari, H., Huss, M., and Zappa, M.: Future shifts in extreme flow regimes in Alpine regions, *Hydrology and Earth System Sciences*, 23, 4471–4489, <https://doi.org/10.5194/hess-23-4471-2019>, 2019a.
- Brunner, M. I., Gurung, A. B., Zappa, M., Zekollari, H., Farinotti, D., and Stähli, M.: Present and future water scarcity in Switzerland: Potential for alleviation through reservoirs and lakes, *Science of the Total Environment*, 666, 1033–1047, <https://doi.org/10.1016/j.scitotenv.2019.02.169>, 2019b.
- 590 Brunner, M. I., Melsen, L. A., Newman, A. J., Wood, A. W., and Clark, M. P.: Future streamflow regime changes in the United States: assessment using functional classification, *Hydrology and Earth System Sciences*, 24, 3951–3966, <https://doi.org/10.5194/hess-24-3951-2020>, 2020.
- Budyko, M.: *Evaporation under natural conditions*, Gidrometeorizdat, Leningrad, English translation by IPST, Jerusalem, 1948.
- Cauvy-Fraunié, S. and Dangles, O.: A global synthesis of biodiversity responses to glacier retreat, *Nature Ecology & Evolution*, 3, 1675–595 1685, <https://doi.org/10.1038/s41559-019-1042-8>, 2019.
- Cramer, W., Yohe, G., Auffhammer, M., Huggel, C., Molau, U., da Silva Dias, M., Solow, A., Stone, D., and Tibig, L.: Detection and attribution of observed impacts., in: *Climate Change 2014: Impacts, Adaptation, and Vulnerability. Part A: Global and Sectoral Aspects. Contribution of Working Group II to the Fifth Assessment Report of the Intergovernmental Panel on Climate Change* [Field, C.B., V.R.



- Barros, D.J. Dokken, K.J. Mach, M.D. Mastrandrea, T.E. Bilir, M. Chatterjee, K.L. Ebi, Y.O. Estrada, R.C. Genova, B. Girma, E.S. Kissel, A.N. Levy, S. MacCracken, P.R. Mastrandrea, and L.L. White (eds.)). Cambridge University Press, Cambridge, United Kingdom and New York, NY, USA, pp. 979–1037, 2014.
- Criss, R. E. and Winston, W. E.: Do Nash values have value? Discussion and alternate proposals, *Hydrological Processes*, 22, 2723–2725, <https://doi.org/10.1002/hyp.7072>, 2008.
- Dobler, C., Bürger, G., and Stötter, J.: Assessment of climate change impacts on flood hazard potential in the Alpine Lech watershed, *Journal of Hydrology*, 460, 29–39, <http://dx.doi.org/10.1016/j.jhydrol.2012.06.027>, 2012.
- Efstratiadis, A. and Koutsoyiannis, D.: One decade of multi-objective calibration approaches in hydrological modelling: a review, *Hydrological Sciences Journal*, 55, 58–78, <https://doi.org/10.1080/02626660903526292>, 2010.
- Euser, T., Winsemius, H., Hrachowitz, M., Fenicia, F., Uhlenbrook, S., and Savenije, H.: A framework to assess the realism of model structures using hydrological signatures, *Hydrology and Earth System Sciences*, 17, <https://doi.org/10.5194/hess-17-1893-2013>, 2013.
- Farinotti, D., Round, V., Huss, M., Compagno, L., and Zekollari, H.: Large hydropower and water-storage potential in future glacier-free basins, *Nature*, 575, 341–344, <https://doi.org/10.1038/s41586-019-1740-z>, 2019.
- Finger, D., Vis, M., Huss, M., and Seibert, J.: The value of multiple data set calibration versus model complexity for improving the performance of hydrological models in mountain catchments, *Water Resources Research*, 51, 1939–1958, <https://doi.org/10.1002/2014WR015712>, 2015.
- Gao, H., Hrachowitz, M., Fenicia, F., Gharari, S., and Savenije, H.: Testing the realism of a topography-driven model (FLEX-Topo) in the nested catchments of the Upper Heihe, China, *Hydrology and Earth System Sciences*, 18, 1895, <https://doi.org/10.5194/hess-18-1895-2014>, 2014.
- Gharari, S., Hrachowitz, M., Fenicia, F., and Savenije, H. H. G.: Hydrological landscape classification: investigating the performance of HAND based landscape classifications in a central European meso-scale catchment, *Hydrology and Earth System Sciences*, 15, 3275–3291, <https://doi.org/10.5194/hess-15-3275-2011>, <https://hess.copernicus.org/articles/15/3275/2011/>, 2011.
- Gharari, S., Hrachowitz, M., Fenicia, F., Gao, H., and Savenije, H.: Using expert knowledge to increase realism in environmental system models can dramatically reduce the need for calibration, *Hydrology and Earth System Sciences*, 18, <https://doi.org/10.5194/hess-18-4839-2015>, 2014.
- Girons Lopez, M., Vis, M. J., Jenicek, M., Griessinger, N., and Seibert, J.: Assessing the degree of detail of temperature-based snow routines for runoff modelling in mountainous areas in central Europe, *Hydrology and Earth System Sciences*, 24, 4441–4461, <https://doi.org/10.5194/hess-24-4441-2020>, 2020.
- Goler, R. A., Frey, S., Formayer, H., and Holzmann, H.: Influence of climate change on river discharge in Austria, *Meteorologische Zeitschrift*, 25, 621–626, <https://doi.org/10.1127/metz/2016/0562>, 2016.
- Hakala, K., Addor, N., Gobbe, T., Ruffieux, J., and Seibert, J.: Risks and opportunities for a Swiss hydroelectricity company in a changing climate, *Hydrology and Earth System Sciences*, 24, 3815–3833, <https://doi.org/10.5194/hess-24-3815-2020>, 2020.
- Hall, D. K. and Riggs, G. A.: MODIS/Terra Snow Cover Daily L3 Global 500m SIN Grid, Version 6., <https://doi.org/10.5067/MODIS/MOD10A1.006>, boulder, Colorado USA. NASA National Snow and Ice Data Center Distributed Active Archive Center., 2016.
- Hanzer, F., Förster, K., Nemeč, J., and Strasser, U.: Projected cryospheric and hydrological impacts of 21st century climate change in the Ötztal Alps (Austria) simulated using a physically based approach, *Hydrology and Earth System Sciences*, 22, 1593–1614, <https://doi.org/10.5194/hess-22-1593-2018>, 2018.



- Her, Y., Yoo, S.-H., Cho, J., Hwang, S., Jeong, J., and Seong, C.: Uncertainty in hydrological analysis of climate change: multi-parameter vs. multi-GCM ensemble predictions, *Scientific Reports*, 9, 1–22, <https://doi.org/10.1038/s41598-019-41334-7>, 2019.
- 640 Holzmann, H., Lehmann, T., Formayer, H., and Haas, P.: Auswirkungen möglicher Klimaänderungen auf Hochwasser und Wasserhaushaltskomponenten ausgewählter Einzugsgebiete in Österreich, *Österreichische Wasser- und Abfallwirtschaft*, 62, 7–14, 2010.
- Hrachowitz, M. and Weiler, M.: Uncertainty of Precipitation Estimates Caused by Sparse Gauging Networks in a Small, Mountainous Watershed, *Journal of Hydrologic Engineering*, 16, 460–471, [https://doi.org/10.1061/\(ASCE\)HE.1943-5584.0000331](https://doi.org/10.1061/(ASCE)HE.1943-5584.0000331), 2011.
- Hrachowitz, M., Fovet, O., Ruiz, L., Euser, T., Gharari, S., Nijzink, R., Freer, J., Savenije, H., and Gascuel-Oudou, C.: Process consistency in models: The importance of system signatures, expert knowledge, and process complexity, *Water Resources Research*, 50, 7445–7469, 645 <https://doi.org/10.1002/2014WR015484>, 2014.
- Hrachowitz, M., Stockinger, M., Coenders-Gerrits, M., van der Ent, R., Bogen, H., Lücke, A., and Stumpp, C.: Deforestation reduces the vegetation-accessible water storage in the unsaturated soil and affects catchment travel time distributions and young water fractions, *Hydrology and Earth System Sciences Discussions*, 2020, 1–43, <https://doi.org/10.5194/hess-2020-293>, <https://hess.copernicus.org/preprints/hess-2020-293/>, 2020.
- 650 Hulsman, P., Savenije, H. H. G., and Hrachowitz, M.: Learning from satellite observations: increased understanding of catchment processes through stepwise model improvement, *Hydrology and Earth System Sciences Discussions*, 2020, 1–26, <https://doi.org/10.5194/hess-2020-191>, <https://hess.copernicus.org/preprints/hess-2020-191/>, 2020.
- Huss, M. and Hock, R.: A new model for global glacier change and sea-level rise, *Frontiers in Earth Science*, 3, 54, <https://doi.org/10.3389/feart.2015.00054>, 2015.
- 655 Immerzeel, W. W., Lutz, A., Andrade, M., Bahl, A., Biemans, H., Bolch, T., Hyde, S., Brumby, S., Davies, B., Elmore, A., et al.: Importance and vulnerability of the world’s water towers, *Nature*, 577, 364–369, <https://doi.org/10.1038/s41586-019-1822-y>, 2020.
- IPCC: Climate Change 2007: The Physical Science Basis. Contribution of Working Group I to the Fourth Assessment Report of the Intergovernmental Panel on Climate Change, [Solomon, S., D. Qin, M. Manning, Z. Chen, M. Marquis, K.B. Averyt, M. Tignor and H.L. Miller (eds.)]. Cambridge University Press, Cambridge, United Kingdom and New York, NY, USA, 996 pp, 2007.
- 660 IPCC: IPCC Special Report on the Ocean and Cryosphere in a Changing Climate, climate [H.-O. Pörtner, D.C. Roberts, V. Masson-Delmotte, P. Zhai, M. Tignor, E. Poloczanska, K. Mintenbeck, A. Alegría, M. Nicolai, A. Okem, J. Petzold, B. Rama, N.M. Weyer (eds.)]. In press, 2019.
- Jacob, D., Petersen, J., Eggert, B., Alias, A., Christensen, O. B., Bouwer, L. M., Braun, A., Colette, A., Déqué, M., Georgievski, G., et al.: EURO-CORDEX: new high-resolution climate change projections for European impact research, *Regional environmental change*, 14, 665 563–578, <https://doi.org/10.1007/s10113-013-0499-2>, 2014.
- Jaramillo, F. and Destouni, G.: Developing water change spectra and distinguishing change drivers worldwide, *Geophysical Research Letters*, 41, 8377–8386, <https://doi.org/10.1002/2014GL061848>, 2014.
- Jenicek, M., Seibert, J., and Staudinger, M.: Modeling of future changes in seasonal snowpack and impacts on summer low flows in alpine catchments, *Water Resources Research*, 54, 538–556, <https://doi.org/10.1002/2017WR021648>, 2018.
- 670 Köplin, N., Schädler, B., Viviroli, D., and Weingartner, R.: Seasonality and magnitude of floods in Switzerland under future climate change, *Hydrological Processes*, 28, 2567–2578, <https://doi.org/10.1002/hyp.9757>, 2014.
- Kormann, C., Francke, T., and Bronstert, A.: Detection of regional climate change effects on alpine hydrology by daily resolution trend analysis in Tyrol, Austria, *Journal of Water and Climate Change*, 6, 124–143, <https://doi.org/10.2166/wcc.2014.099>, 2015.



- Laaha, G., Parajka, J., Viglione, A., Koffler, D., Haslinger, K., Schöner, W., Zehetgruber, J., and Blöschl, G.: A three-pillar approach to
675 assessing climate impacts on low flows, *Hydrology and Earth System Sciences*, 20, 3967, <https://doi.org/10.5194/hess-20-3967-2016>,
2016.
- Laghari, A., Vanham, D., and Rauch, W.: To what extent does climate change result in a shift in Alpine hydrology? A case study in the
Austrian Alps, *Hydrological Sciences Journal*, 57, 103–117, <https://doi.org/10.1080/02626667.2011.637040>, 2012.
- Lambrecht, A. and Kuhn, M.: Glacier changes in the Austrian Alps during the last three decades, derived from the new Austrian glacier
680 inventory, *Annals of Glaciology*, 46, 177–184, <https://doi.org/10.3189/172756407782871341>, 2007.
- Laurent, L., Buoncristiani, J.-F., Pohl, B., Zekollari, H., Farinotti, D., Huss, M., Mugnier, J.-L., and Pergaud, J.: The impact of climate change
and glacier mass loss on the hydrology in the Mont-Blanc massif, *Scientific Reports*, 10, 1–11, <https://doi.org/10.1038/s41598-020-67379-7>, 2020.
- MacDonald, M., Pomeroy, J., and Pietroniro, A.: On the importance of sublimation to an alpine snow mass balance in the Canadian Rocky
685 Mountains, *Hydrology and Earth System Sciences*, 14, 1401, <https://doi.org/10.5194/hess-14-1401-2010>, 2010.
- Mader, H., Steidl, T., and Wimmer, R.: *Abflußregime österreichischer Fließgewässer*, Wien, AUT: Umweltbundesamt, 1996.
- Mankin, J. S., Viviroli, D., Mekonnen, M. M., Hoekstra, A. Y., Horton, R. M., Smerdon, J. E., and Diffenbaugh, N. S.: Influence of internal
variability on population exposure to hydroclimatic changes, *Environmental Research Letters*, 12, 044 007, <https://doi.org/10.1088/1748-9326/aa5efc>, 2017.
- 690 Marty, C., Schlogl, S., Bavay, M., and Lehning, M.: How much can we save? Impact of different emission scenarios on future snow cover in
the Alps, *The Cryosphere*, 11, 517–529, <https://doi.org/10.1088/1748-9326/aa5efc>, 2017.
- Marx, A., Kumar, R., Thober, S., Rakovec, O., Wanders, N., Zink, M., Wood, E. F., Pan, M., Sheffield, J., and Samaniego, L.: Climate
change alters low flows in Europe under global warming of 1.5, 2, and 3 C, *Hydrology and Earth System Sciences*, 22, 1017–1032,
<https://doi.org/10.5194/hess-22-1017-2018>, 2018.
- 695 Merz, R. and Blöschl, G.: A process typology of regional floods, *Water Resources Research*, 39, <https://doi.org/10.1029/2002WR001952>,
2003, 2003.
- Mostbauer, K., Kaitna, R., Prenner, D., and Hrachowitz, M.: The temporally varying roles of rainfall, snowmelt and soil moisture for debris
flow initiation in a snow-dominated system, *Hydrology and Earth System Sciences*, 22, 3493–3513, <https://doi.org/10.5194/hess-22-3493-2018>, 2018.
- 700 Muelchi, R., Rössler, O., Schwanbeck, J., Weingartner, R., and Martius, O.: Future runoff regime changes and their time of emergence for
93 catchments in Switzerland, *Hydrology and Earth System Sciences Discussions*, 2020, 1–25, <https://doi.org/10.5194/hess-2020-516>,
<https://hess.copernicus.org/preprints/hess-2020-516/>, in review, 2020.
- Muelchi, R., Rössler, O., Schwanbeck, J., Weingartner, R., and Martius, O.: Moderate runoff extremes in Swiss rivers and their seasonal
occurrence in a changing climate, *Hydrology and Earth System Sciences Discussions*, <https://doi.org/10.5194/hess-2020-667>, in review,
705 2021.
- Nash, J. E. and Sutcliffe, J. V.: River flow forecasting through conceptual models part I—A discussion of principles, *Journal of Hydrology*,
10, 282–290, 1970.
- Nijzink, R., Hutton, C., Pechlivanidis, I., Capell, R., Arheimer, B., Freer, J., Han, D., Wagener, T., McGuire, K., Savenije, H., and Hra-
chowicz, M.: The evolution of root-zone moisture capacities after deforestation: a step towards hydrological predictions under change?,
710 *Hydrology and Earth System Sciences*, 20, 4775–4799, <https://doi.org/10.5194/hess-20-4775-2016>, <https://hess.copernicus.org/articles/20/4775/2016/>, 2016.



- Oudin, L., Hervieu, F., Michel, C., Perrin, C., Andréassian, V., Anctil, F., and Loumagne, C.: Which potential evapotranspiration input for a lumped rainfall–runoff model?: Part 2—Towards a simple and efficient potential evapotranspiration model for rainfall–runoff modelling, *Journal of Hydrology*, 303, 290–306, <https://doi.org/10.1016/j.jhydrol.2004.08.026>, 2005.
- 715 Parajka, J., Kohnová, S., Merz, R., Szolgay, J., Hlavčová, K., and Blöschl, G.: Comparative analysis of the seasonality of hydrological characteristics in Slovakia and Austria/Analyse comparative de la saisonnalité de caractéristiques hydrologiques en Slovaquie et en Autriche, *Hydrological Sciences Journal*, 54, 456–473, <https://doi.org/10.1623/hysj.54.3.456>, 2009.
- Parajka, J., Kohnová, S., Bálint, G., Barbuc, M., Borga, M., Claps, P., Cheval, S., Dumitrescu, A., Gaume, E., Hlavčová, K., et al.: Seasonal characteristics of flood regimes across the Alpine–Carpathian range, *Journal of hydrology*, 394, 78–89, <https://doi.org/10.1016/j.jhydrol.2010.05.015>, 2010.
- 720 Parajka, J., Blaschke, A. P., Blöschl, G., Haslinger, K., Hepp, G., Laaha, G., Schöner, W., Trautvetter, H., Viglione, A., and Zessner, M.: Uncertainty contributions to low-flow projections in Austria, *Hydrology and Earth System Sciences*, 20, 2085, <https://doi.org/10.5194/hess-20-2085-2016>, 2016.
- Prenner, D., Kaitna, R., Mostbauer, K., and Hrachowitz, M.: The value of using multiple hydrometeorological variables to predict temporal debris flow susceptibility in an alpine environment, *Water Resources Research*, 54, 6822–6843, <https://doi.org/10.1029/2018WR022985>, 2018.
- 725 Prenner, D., Hrachowitz, M., and Kaitna, R.: Trigger characteristics of torrential flows from high to low alpine regions in Austria, *Science of The Total Environment*, 658, 958–972, <https://doi.org/10.1016/j.scitotenv.2018.12.206>, 2019.
- Roodari, A., Hrachowitz, M., Hassanpour, F., and Yaghoobzadeh, M.: Signatures of human intervention – or not? Downstream intensification of hydrological drought along a large Central Asian River: the individual roles of climate variability and land use change, *Hydrology and Earth System Sciences Discussions*, 2020, 1–40, <https://doi.org/10.5194/hess-2020-369>, <https://hess.copernicus.org/preprints/hess-2020-369/>, 2020.
- 730 Savenije, H. H.: HESS Opinions "Topography driven conceptual modelling (FLEX-Topo)", *Hydrology and Earth System Sciences*, 14, 2681, <https://doi.org/10.5194/hess-14-2681-2010>, 2010.
- 735 Schaepli, B., Manso, P., Fischer, M., Huss, M., and Farinotti, D.: The role of glacier retreat for Swiss hydropower production, *Renewable Energy*, 132, 615–627, <https://doi.org/10.1016/j.renene.2018.07.104>, 2019.
- Schneeberger, K., Dobler, C., Huttenlau, M., and Stötter, J.: Assessing potential climate change impacts on the seasonality of runoff in an Alpine watershed, *Journal of Water and Climate Change*, 6, 263–277, <https://doi.org/10.2166/wcc.2014.106>, 2015.
- Seibert, J. and Vis, M. J.: Teaching hydrological modeling with a user-friendly catchment-runoff-model software package, *Hydrology and Earth System Sciences*, 16, 3315–3325, <https://doi.org/10.5194/hess-16-3315-2012>, 2012.
- 740 Seiller, G. and Anctil, F.: How do potential evapotranspiration formulas influence hydrological projections?, *Hydrological Sciences Journal*, 61, 2249–2266, <https://doi.org/10.1080/02626667.2015.1100302>, 2016.
- Stanzel, P. and Nachtnebel, H.: Mögliche Auswirkungen des Klimawandels auf den Wasserhaushalt und die Wasserkraftnutzung in Österreich, *Österreichische Wasser-und Abfallwirtschaft*, 62, 180–187, 2010.
- 745 Switanek, M. B., Troch, P. A., Castro, C. L., Leuprecht, A., Chang, H.-I., Mukherjee, R., and Demaria, E. M.: Scaled distribution mapping: a bias correction method that preserves raw climate model projected changes, *Hydrology and Earth System Sciences*, 21, 2649–2649, <https://doi.org/10.5194/hess-21-2649-2017>, 2017.
- Switanek, M. B., Maraun, D., and Bevacqua, E.: Stochastic downscaling of gridded precipitation to spatially coherent sub-grid precipitation fields using a transformed Gaussian model, in preparation, 2021.



- 750 Tecklenburg, C., Francke, T., Kormann, C., and Bronstert, A.: Modeling of water balance response to an extreme future scenario in the Ötztal catchment, Austria, *Advances in Geosciences*, 32, 63–68, <https://doi.org/10.5194/adgeo-32-63-2012>, 2012.
- Thielen, A. H., Cammerer, H., Dobler, C., Lammel, J., and Schöberl, F.: Estimating changes in flood risks and benefits of non-structural adaptation strategies—a case study from Tyrol, Austria, *Mitigation and Adaptation Strategies for Global Change*, 21, 343–376, <https://doi.org/10.1007/s11027-014-9602-3>, 2016.
- 755 Thober, S., Kumar, R., Wanders, N., Marx, A., Pan, M., Rakovec, O., Samaniego, L., Sheffield, J., Wood, E. F., and Zink, M.: Multi-model ensemble projections of European river floods and high flows at 1.5, 2, and 3 degrees global warming, *Environmental Research Letters*, 13, 014 003, <https://doi.org/10.1088/1748-9326/aa9e35>, 2018.
- Thornthwaite, C. W.: An approach toward a rational classification of climate, *Geographical Review*, 38, 55–94, 1948.
- Viviroli, D., Dürr, H. H., Messerli, B., Meybeck, M., and Weingartner, R.: Mountains of the world, water towers for humanity: Typology, mapping, and global significance, *Water Resources Research*, 43, <https://doi.org/10.1029/2006WR005653>, 2007.
- 760 Vormoor, K., Lawrence, D., Heistermann, M., and Bronstert, A.: Climate change impacts on the seasonality and generation processes of floods—projections and uncertainties for catchments with mixed snowmelt/rainfall regimes., *Hydrology & Earth System Sciences*, 19, <https://doi.org/10.5194/hess-19-913-2015>, 2015.
- Vormoor, K., Rössler, O., Bürger, G., Bronstert, A., and Weingartner, R.: When timing matters—considering changing temporal structures in runoff response surfaces, *Climatic Change*, 142, 213–226, <https://doi.org/10.1007/s10584-017-1940-1>, 2017.
- 765 Young, A., Round, C., and Gustard, A.: Spatial and temporal variations in the occurrence of low flow events in the UK, *Hydrology and Earth System Sciences*, 4, 35–45, 2000.
- Zekollari, H., Huss, M., and Farinotti, D.: Modelling the future evolution of glaciers in the European Alps under the EURO-CORDEX RCM ensemble, *The Cryosphere*, 13, 1125–1146, <https://doi.org/10.5194/tc-13-1125-2019>, 2019.